© 2019. Published by The Company of Biologists Ltd | Development (2019) 146, dev174243. doi:10.1242/dev.174243

RESEARCH ARTICLE

Dmrt factors determine the positional information of cerebral cortical progenitors via differential suppression of homeobox genes

Daijiro Konno[1,2,‡], Chiaki Kishida[1,*], Kazumitsu Maehara[3], Yasuyuki Ohkawa[3], Hiroshi Kiyonari[4], Seiji Okada[2] and Fumio Matsuzaki[1,‡]

ABSTRACT

The spatiotemporal identity of neural progenitors and the regional control of neurogenesis are essential for the development of cerebral cortical architecture. Here, we report that mammalian DM domain factors (Dmrt) determine the identity of cerebral cortical progenitors. Among the Dmrt family genes expressed in the developing dorsal telencephalon, *Dmrt3* and *Dmrta2* show a medial^{high}/lateral^{low} expression gradient. Their simultaneous loss confers a ventral identity to dorsal progenitors, resulting in the ectopic expression of Gsx2 and massive production of GABAergic olfactory bulb interneurons in the dorsal telencephalon. Furthermore, double-mutant progenitors in the medial region exhibit upregulated Pax6 and more lateral characteristics. These ventral and lateral shifts in progenitor identity depend on Dmrt gene dosage. We also found that Dmrt factors bind to *Gsx2* and *Pax6* enhancers to suppress their expression. Our findings thus reveal that the graded expression of Dmrt factors provide positional information for progenitors by differentially repressing downstream genes in the developing cerebral cortex.

KEY WORDS: LGE, Cerebral cortex, Dorsoventral patterning, Neural progenitor, Neurogenesis, Olfactory bulb, Mouse

INTRODUCTION

During the development of the central nervous system, neural progenitors acquire regionally restricted properties that enforce a unique identity on their neuronal progeny. These properties, which determine progenitor identity, are involved not only in the determination of the fate of their progeny but also in the spatiotemporal patterns of cell cycle progression, division mode, and neurogenic ability (Martynoga et al., 2012; Paridaen and Huttner, 2014).

The telencephalon is the most anterior region of the developing central nervous system. It comprises the dorsal telencephalon (pallium) and ventral telencephalon (subpallium). The dorsal telencephalon gives rise to the cerebral cortex and the hippocampus by the spatial and temporal regulation of secreted inductive signals to provide positional information that defines progenitor identity. The initial step of cerebral cortical development requires reciprocal and/or independent action of extrinsic factors, such as Bmps, Fgfs, Shh and Wnts, which are secreted from signaling centers in the developing telencephalon (Hoch et al., 2009). In addition, many transcription factors have been identified as downstream targets of these extrinsic factors (Hébert and Fishell, 2008). These effectors in turn specify regional cell types and the neurogenic potential of progenitors. Among such factors, the transcription factors Pax6 and Gli3 play an essential role in the acquisition and maintenance of neural progenitor identity in the developing dorsal telencephalon (Grove et al., 1998; Kroll and O'Leary, 2005; Kuschel et al., 2003; Stoykova et al., 2000; Theil et al., 1999; Tole et al., 2000b; Toresson et al., 2000; Yun et al., 2001). In mice lacking *Pax6* or *Gli3*, the dorsal-ventral (D-V) boundary is severely disorganized, resulting in the ectopic expression of several ventral-specific transcription factors, such as Gsx2 (also called Gsh2), Ascl1 (also called Mash1), and Dlxs, which are involved in the specification of all GABAergic interneurons in the ventral telencephalon (Long et al., 2009; Wang et al., 2013). However, the additional knockout of *Shh* in mice lacking *Pax6* or *Gli3* can partly rescue the disorganization of the D-V boundary (Aoto et al., 2002; Fuccillo et al., 2006; Rallu et al., 2002; Rash and Grove, 2007), raising the possibility that there are unknown factors that are required for the determination of the identity of cerebral cortex progenitors.

The neurogenic ability of neural progenitors is also dynamically controlled by spatial and temporal information during cortical development. At the early stages of cortical development, neural progenitors are proliferative, undergoing symmetric cell divisions. In contrast, at later stages, progenitors gradually mature to generate cortical neurons. The spatiotemporal control of the transition of progenitors from a less to a more neurogenic state provides a basis for establishing the complex architecture of the cerebral cortex. D-V patterning factors, such as Shh and Pax6, play central roles in regulating the neurogenic ability of progenitors in the developing cerebral cortex. These factors regulate neurogenesis in part by cooperating with the Notch-Delta signaling pathway, which promotes self-renewal of neural progenitors (Dave et al., 2011; Sansom et al., 2009). However, it remains unclear how the neurogenic ability of cortical neural progenitors are spatiotemporally controlled during development.

Here, we report that three mammalian DM domain (Dmrt) factors, Dmrt3, Dmrta1 (also called Dmrt4) and Dmrta2 (also called Dmrt5) determine the identity of cerebral cortical progenitors and regulate the neurogenic ability of these cells in developing mouse embryos. We provide evidence that low levels of Dmrt factors repress *Gsx2* expression in the dorsal telencephalon, thereby

[1]Laboratory for Cell Asymmetry, RIKEN Center for Biosystems Dynamics Research, Kobe, Hyogo 650-0047, Japan. [2]Division of Pathophysiology, Medical Institute of Bioregulation, Kyushu University, Fukuoka 812-8582, Japan. [3]Division of Transcriptomics, Medical Institute of Bioregulation, Kyushu University, Fukuoka 812-8582, Japan. [4]Laboratories for Animal Resource Development and Genetic Engineering (LARGE), RIKEN Center for Biosystems Dynamics Research, Kobe, Hyogo 650-0047, Japan.
*Present address: Department of Molecular, Cell and Systems Biology, University of California, Riverside, CA 92521, USA.

‡Authors for correspondence (dai-kon@umin.ac.jp; fumio@cdb.riken.jp)

D.K., 0000-0002-1387-7528; K.M., 0000-0002-2933-5176; Y.O., 0000-0001-6440-9954; F.M., 0000-0001-7902-4520

Received 26 November 2018; Accepted 23 July 2019

Development (2019) 146, dev174243. doi:10.1242/dev.174243

defining the pallial-subpallial boundary and specifying neural progenitors that produce glutamatergic neurons. Moreover, a graded expression of Dmrt factors suppresses *Pax6* transcription and establishes a medial^{low}/lateral^{high} Pax6 expression gradient. In this way, a neurogenic gradient is formed in the developing cerebral cortex.

RESULTS

Dmrt factors maintain the dorsal-ventral patterning of the telencephalon

We first examined the precise expression patterns of Dmrt3 and Dmrta2, which are the predominant Dmrt factors in the developing dorsal telencephalon of rodents (Fig. S1A-C). Whole-mount immunofluorescence was performed on embryonic day (E) 9.5 mouse embryos, in which the dorsal-ventral patterning of the telencephalon had just been established. In these embryos, Dmrt3 and Dmrta2 were detected predominantly in the telencephalon (Fig. S1D). At E12.5, Dmrt3 and Dmrta2 were detected in a restricted pattern in the dorsal telencephalon, with a medial^{high}/lateral^{low} gradient (Fig. S1E). Quantitative RT-PCR (qRT-PCR) analysis confirmed that *Dmrt3* and *Dmrta2* transcripts were predominantly expressed in the medial telencephalon, and no differences in their expression were observed along the anterior-posterior axis (Fig. S1F-H).

We and others have previously reported that *Dmrta2* single mutants exhibit a reduction in size of the dorsal telencephalon, with the complete loss of medial regions, such as the cortical hem (Konno et al., 2012; Saulnier et al., 2013). To test whether the Dmrt factors have overlapping roles, we fist examined *Dmrt3* and *Dmrta2* double mutants. *Dmrt3*$^{-/-}$;*Dmrta2*$^{-/-}$ mutant mice died soon after birth. At E15.5, the telencephalon of *Dmrt3*$^{-/-}$;*Dmrta2*$^{-/-}$ embryos appeared smaller in size compared with control embryos (Fig. 1A, Fig. S1I). Immunostaining for Gad2, an enzyme involved in GABA synthesis, revealed ectopic production of GABAergic neurons in the dorsal telencephalon of *Dmrt3*$^{-/-}$;*Dmrta2*$^{-/-}$ mutant embryos (Fig. 1B, Fig. S1J). Concomitantly, the production of cortical excitatory neurons, labeled with Tbr1 (cortical deep layer neurons) or Pou3f2 (also called Brn-2; cortical upper layer neurons), was markedly decreased in the dorsal telencephalon of mutant embryos (Fig. 1B, Fig. S1J). These results indicate that the Dmrt factors are involved in determining the identity of neurons generated in the dorsal telencephalon.

We next asked whether the D-V patterning in the mutant telencephalon was affected at the progenitor level. *Dmrt3*$^{-/-}$;*Dmrta2*$^{-/-}$ E12.5 embryos showed a marked reduction in size of the telencephalon, with no prominent defects in other CNS regions (Fig. 1C) (data not shown). The expression of the transcriptional factor Gsx2 is restricted in ventral telencephalic progenitors (subpallium) in wild-type embryos. However, this factor was observed ectopically in the dorsal telencephalon of double-mutant embryos, suggesting a ventral shift in cortical progenitor fate in the mutant embryos. Consistent with this finding, transcription factors

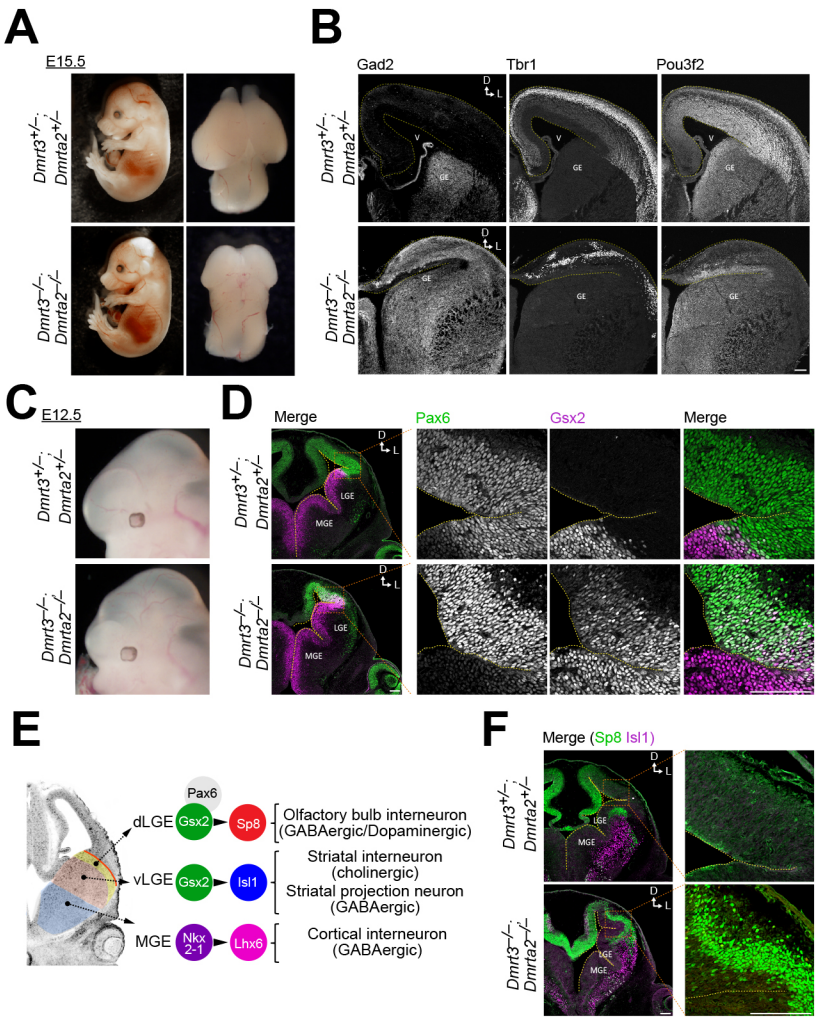

Fig. 1. Disorganization of cerebral cortical development in Dmrt mutant embryos. (A) Lateral views (left) and top views of the forebrain (right) of E15.5 *Dmrt3*/*Dmrta2* double-mutant embryos. (B) Immunofluorescence for Gad2, Tbr1 and Pou3f2 in coronal sections of the telencephalon in *Dmrt3*/*Dmrta2* mutant E15.5 embryos. (C) Lateral views of the head region in *Dmrt3*/*Dmrta2* mutant E12.5 embryos. (D) Immunofluorescence for Pax6 and Gsx2 in coronal sections of the telencephalon of *Dmrt3*/*Dmrta2* mutant E12.5 embryos. (E) Schematic of the transcriptional cascade giving rise to distinct neuronal subtypes in the nascent ventral telencephalon. (F) Immunofluorescence for Sp8 and Isl1 in coronal sections of the telencephalon of *Dmrt3*/*Dmrta2* mutant E12.5 embryos. In D and F, the right panels represent higher magnifications of the boxed regions indicated in the left panels. D, dorsal; GE, ganglionic eminence; L, lateral; LGE, lateral ganglionic eminence; MGE, medial ganglionic eminence; V, ventricle. In all immunofluorescence images, the yellow dotted lines indicate the ventricular surface. Scale bars: 100 µm.

Development (2019) 146, dev174243. doi:10.1242/dev.174243

involved in generating cortical excitatory neurons, such as Emx1, Neurog2 and Tbr2 (Eomes), exhibited markedly decreased expression in the mutant dorsal telencephalon (Fig. S2A,B). Interestingly, the expression of Pax6, a transcription factor involved in the development of the dorsal telencephalon, was maintained in the mutant embryos, resulting in the simultaneous expression of Gsx2 and Pax6 in these neural progenitors (Fig. 1D, Fig. S1K).

In wild-type embryos, Gsx2 and Pax6 are co-expressed in a small subset of neural progenitors in the dorsal-most aspect of the ventral telencephalon, which comprises the pallial-subpallial boundary (PSB, or the boundary between the dorsal and ventral telencephalon) and the dorsal lateral ganglionic eminence (dLGE) (Corbin et al., 2003; Toresson et al., 2000; Yun et al., 2001). This region gives rise to olfactory bulb interneurons by activating the expression of the transcription factor Sp8 (Fig. 1E) (Waclaw et al., 2006). This Gsx2-Pax6 double-positive region is adjacent to the ventral LGE (vLGE), which expresses Gsx2 but not Pax6. The vLGE generates striatal neurons that express Isl1 (Ehrman et al., 2013), another downstream transcription factor known to be regulated by Gsx2. To identify subtypes of neurons generated in the mutant dorsal telencephalon that express both Gsx2 and Pax6 in progenitors, we examined the expression of Sp8 and Isl1 in the double-mutant embryos, and found that they ectopically express Sp8 but not Isl1 in the dorsal telencephalon (Fig. 1F, Fig. S1L), suggesting that the simultaneous depletion of Dmrt3 and Dmrta2 expands the PSB/dLGE more dorsally by converting the identity of the cortical progenitors to that of the PSB and/or dLGE. This result was confirmed by the persistent expression of Pax6, a marker of migrating olfactory bulb (OB) interneurons, in the cells that migrate anteriorly (Fig. S3A). Thus, the expression of Dmrt genes appears to be involved in determining the position and size of PSB/dLGE, the region between the dorsal and ventral telencephalon (pallium and subpallium) along the dorsoventral axis.

Gene dosage-dependent suppression of OB neurons by Dmrt factors

As the expression of Dmrta2 and Dmrt3 exhibits a graded pattern along the lateral-dorsal-medial axis, our results regarding the role of Dmrts on the determination of differential progenitor identity suggest that Dmrt gene dosage affects the position and the size of PSB/dLGE. If so, then Dmrt dosage would consequently alter the relative number different neuronal subtypes. We tested this possibility by examining the proportion of OB projection neurons (OB-p) and OB interneurons (OB-i), which are produced from the dorsal and ventral domains adjacent to the PSB, respectively (Ceci et al., 2012; Wichterle et al., 1999), in mice with various dosage combinations of Dmrt genes. These neurons migrate anteriorly to form the olfactory cortex and are distinguishable by several markers. Specifically, subsets of OB-i are characterized by tyrosine hydroxylase expression, whereas OB-p neurons can be identified by calretinin (calbindin 2) expression (Fig. 2A,B) (Waclaw et al., 2006). In *Dmrt3*$^{+/-}$;*Dmrta2*$^{+/-}$ control embryos, the OB-i and OB-p domains formed adequately in the anterior border of the telencephalon at E12.5, whereas *Dmrt3*$^{-/-}$;*Dmrta2*$^{+/-}$ or *Dmrta2*$^{-/-}$ embryos exhibited a slight expansion of the OB-i domain (Fig. 2C-E). Interestingly, a more significant expansion of the OB-i was seen in *Dmrt3*$^{+/-}$;*Dmrta2*$^{-/-}$ embryos, and the most striking effect was observed in *Dmrt3*$^{-/-}$;*Dmrta2*$^{-/-}$ embryos. This effect occurred in association with no significant expansion of the OB-p domain (calretinin positive) and the gradual decrease of the cerebral cortical domain (calretinin/TH double negative) (Fig. 2F, G). These observations are consistent with Dmrt factor dosage determining the relative proportions of the primordium of the OB and the cerebral cortex (see also Fig. S3A,B).

We next addressed the role of the other Dmrt factor, Dmrta1, which is expressed nearly uniformly in the anterior dorsal telencephalon and in a medial^{low}/lateral^{high} gradient in the posterior dorsal telencephalon (Fig. S4A-C). Although *Dmrta1*$^{-/-}$

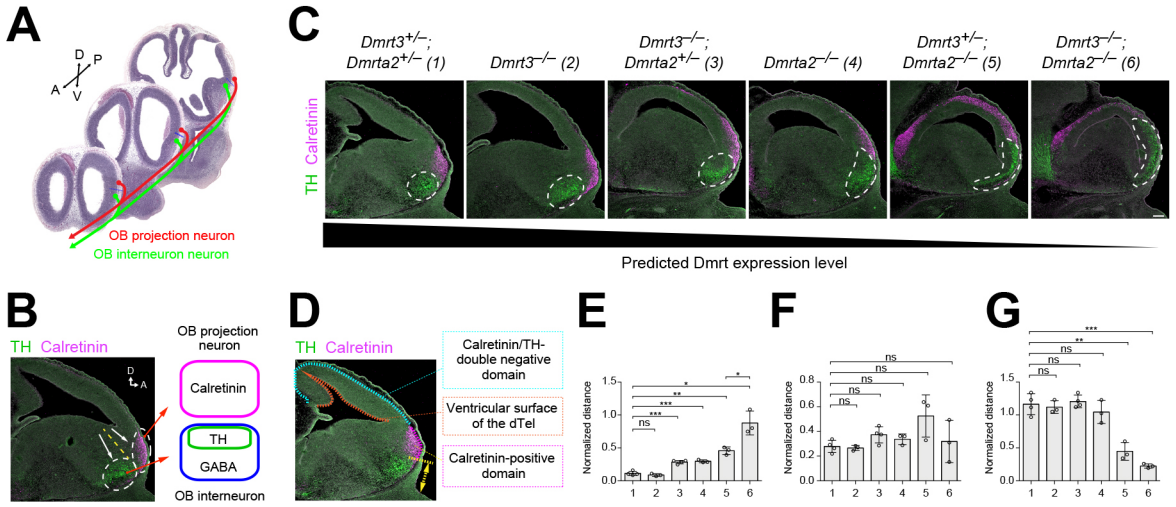

Fig. 2. Gene dosage-dependent suppression of OB neurons by Dmrt factors. (A) Schematic of the production of the OB projection and interneurons from the telencephalic regions near the PSB at E12.5. Section images of Hematoxylin and Eosin staining are from the public database EPMBA (http://www.epmba.org). A, anterior; D, dorsal; P, posterior; V, ventral. (B) Detection of early OB neuron production with calretinin and tyrosine hydroxylase (TH) in a sagittal section of the developing mouse telencephalon at E12.5. (C) Immunofluorescence for calretinin and TH in sagittal sections of the telencephalon from the various combinations of mutants for Dmrt3 and Dmrta2 at E12.5. Dashed line encircles the TH-positive domain. (D-G) Quantification of the distance from the base of the nasal process to the distal end of the TH-positive domain (yellow line; E), the size of the calretinin-positive domain (magenta line; F), and the size of calretinin/TH-double negative (cortical) domain (light blue line; G) normalized to the length of the dorsal ventricular surface (red line). The panel in D displays how the distance and the size of each domain were measured. Numbers below the graphs in E-G correspond to the numbers next to the genotypes in C. The error bars represent ±s.d. [n=4 per group (samples #1 and 3), n=3 per group (samples #2, #4, #5, #6)]. Statistical significance was determined using Student's t-test with Welch's correction (ns, not significant; *P<0.05; **P<0.01; ***P<0.001). Scale bars: 100 µm.

Development (2019) 146, dev174243. doi:10.1242/dev.174243

mutant embryos exhibited no clear abnormalities (Fig. S4D-F), knocking out *Dmrta1* in *Dmrta2*$^{-/-}$ mice resulted in a marked upregulation of Gsx2 expression in the dorsal telencephalon at E12.5, resembling the phenotype observed in *Dmrt3*$^{-/-}$;*Dmrta2*$^{-/-}$ embryos (Fig. S4G). *Dmrt3*$^{-/-}$;*Dmrta2*$^{-/-}$;*Dmrta1*$^{-/-}$ embryos also exhibited ectopic expression of Gsx2 similar to those observed in *Dmrta1*$^{-/-}$;*Dmrta2*$^{-/-}$ or *Dmrt3*$^{-/-}$;*Dmrta2*$^{-/-}$ embryos (Fig. S4H). These results suggest that all Dmrt 'A' factors work along the same molecular pathway in the developing cerebral cortex.

Cell-autonomous suppression of ventral cell fate by Dmrt factors

We next examined whether and how the loss of Dmrt factor function affects neighboring cells. To this end, we generated chimeric mutant embryos by injecting *Dmrt3*$^{-/-}$;*Dmrta2*$^{-/-}$;*Dmrta1*$^{-/-}$ (TKO) embryonic stem (ES) cells into wild-type blastocysts. Whereas *Dmrt3*$^{-/-}$;*Dmrta2*$^{-/-}$ embryos showed a slight increase in the expression of Gsx2 at the most lateral portion of the dorsal telencephalon at E10.5, TKO chimeric mutant embryos showed a strong expression of Gsx2 over the entire region of the dorsal telencephalon (Fig. 3A). Ectopic expression of Sp8 was also observed to a greater extent in TKO chimeric embryos than in double knockout (DKO) embryos (Fig. 3B). Notably, ectopic Gsx2 expression in the dorsal telencephalon of TKO chimeric embryos was observed only in cells lacking Dmrt factors (Fig. 3A), indicating their cell-autonomous function.

Dmrt factors repress the expression of several ventral genes

Given that all Dmrt factors contain an intertwined zinc finger-like DNA-binding module, the DM domain (Fig. S1A,B), we next sought to reveal the transcriptional network that is regulated by Dmrt3 and Dmrta2 (Fig. 4A). Transcriptomic analysis of the *Dmrt3*$^{-/-}$;*Dmrta2*$^{-/-}$ dorsal telencephalon at E12.5 showed significant upregulation of many genes involved in differentiation and patterning of neural progenitors in the ventral telencephalon (Fig. 4B). This result is consistent with the ventral conversion of dorsal (cortical) progenitors and the ectopic production of GABAergic neurons described above. *Dmrt3*$^{+/-}$;*Dmrta2*$^{-/-}$ embryos also showed a similar phenotype but to a lesser extent than *Dmrt3*$^{-/-}$;*Dmrta2*$^{-/-}$ embryos, indicating that Dmrt function is also dosage dependent at the transcriptome level (Fig. 4B). As a first step to identify direct targets of Dmrt factors, we compared the effects of constitutive Dmrt factor knockout (Fig. 4B) with those of acute loss of function by introducing siRNAs via *in utero* electroporation into the dorsolateral telencephalon (Fig. 4C, Fig. S5A, B). Intriguingly, among the top 30 upregulated genes, only *Gsx2* and its protein product were markedly upregulated in the cells electroporated with siRNAs targeting *Dmrta2* and *Dmrt3* (or *Dmrta1*) (hereafter termed DKD cells) (Fig. 4D,E, Fig. S6A,B). By contrast, the expression of other genes, such as *Dlx1*, a transcription factor controlling differentiation of GABAergic neurons (Anderson et al., 1999), *Neurog2* and *Ascl1* was changed in DKD cells (*Dlx1*: 3.8-fold increase, *Ascl1*: 1.5-fold increase, *Pax6*: 1.3-fold increase, and *Neurog2*: 1.1-fold decrease, versus control); however, the rate of change was over 18-fold lower than that for *Gsx2* (68.8-fold increase versus control) (Fig. 4D,E). This finding raises the possibility that *Gsx2* is a downstream target of Dmrt factors. An exogenously expressed fusion protein of the DM domain and the VP16 transcriptional activation domain also induced ectopic expression of *Gsx2* and its protein product in the electroporated cells (Fig. S7A-C), suggesting that Dmrt factors function as transcriptional repressors for *Gsx2* expression.

Given that sonic hedgehog (Shh) is a central mediator of D-V patterning at the onset of neural development (Dessaud et al., 2008), we tested for a functional interaction between Shh signaling and Dmrt. No significant changes in the expression levels of genes involved in the Shh signaling pathway, such as *Gli1* and *Ptch1*, were observed in DKD cells (Fig. S8A). In addition, neither the presence nor the absence of Dmrta2 affected transcriptional activation by Gli2 or repression by Gli3R (a repressor form of Gli3) in the Shh-reporter assay (Fig. S8B). These results suggest that Dmrt3 and Dmrta2 act in the D-V patterning of the telencephalon independently of Shh signaling.

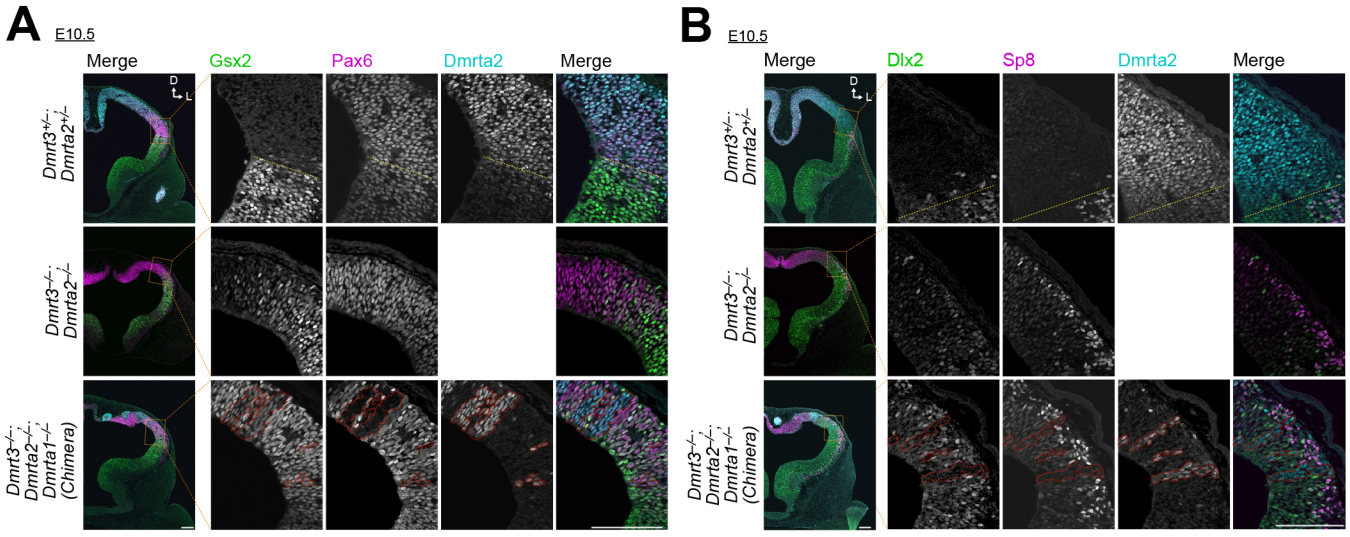

Fig. 3. Cell-autonomous suppression of the ventral cell fate by Dmrt. (A) Immunofluorescence for Gsx2, Pax6 and Dmrta2 in coronal sections of the E10.5 mouse telencephalon. Sections are from *Dmrt3*/*Dmrta2* double-mutant embryos (top and middle) or *Dmrt3*/*Dmrta2*/*Dmrta1* triple-mutant embryos (bottom) established by blastocyst injection of *Dmrt3*/*Dmrta1*/*Dmrta2* TKO ES cells to generate chimeras. (B) Immunofluorescence for Sp8, Dlx2 and Dmrta2 in coronal sections of the E10.5 mouse telencephalon of *Dmrt3*/*Dmrta2* double-mutant embryos (top and middle) or *Dmrt3*/*Dmrta2*/*Dmrta1* triple-mutant embryos (chimera, bottom). The yellow dotted lines indicate the ventricular surface. The red lines indicate Dmrta2-positive wild-type-derived cells in the TKO chimeric embryo. Scale bars: 100 µm.

Development (2019) 146, dev174243. doi:10.1242/dev.174243

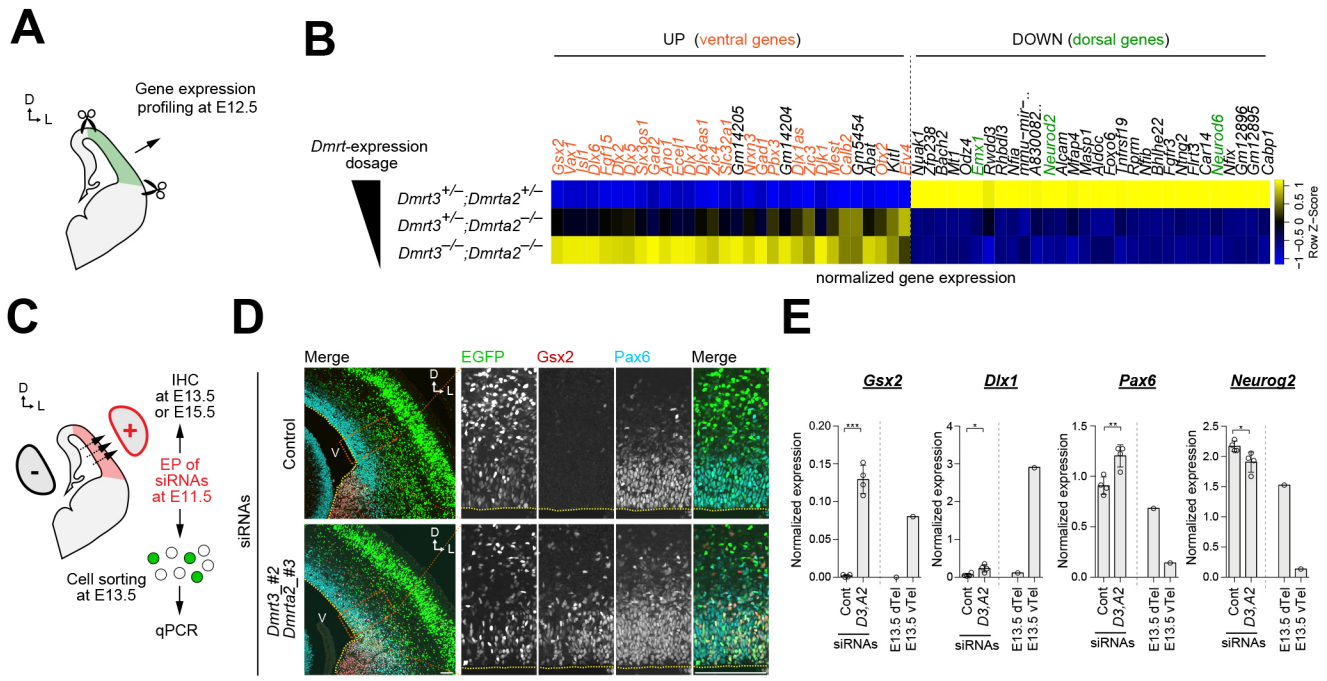

Fig. 4. Repression of telencephalic ventral genes by Dmrt factors. (A) Schematic of the experimental design for gene expression profiling of Dmrt mutant brains. (B) Transcriptome analysis in the dorsolateral telencephalon of Dmrt double-mutant E12.5 embryos. The heat-maps reflect normalized gene expression. Genes that have been reported as ventral and dorsal specific are indicated in orange and green, respectively. (C) Schematic summarizing the experimental design for histological (D) and gene expression (E) analyses based on siRNA treatment of developing mouse embryos. siRNAs were electroporated with the EGFP-NLS expression vector in the dorsolateral cortex at E11.5. (D) Immunofluorescence for Gsx2 and Pax6 and EGFP fluorescence in coronal sections of the E15.5 mouse telencephalon electroporated with control siRNAs (top) or siRNAs targeting *Dmrt3* and *Dmrta2* (bottom). The right panels represent higher magnifications of the boxed regions indicated in the left panels. The yellow dotted lines indicate the ventricular surface. Scale bars: 100 µm. (E) Gene expression of *Gsx2*, *Dlx1*, *Pax6* and *Neurog2* normalized to *Sox2* in the control (lane 1) or double-knockdown (D3/A2, lane 2) cells, as determined by qPCR. The E13.5 dorsal and ventral telencephalon [dTel (lane 3) and vTel (lane 4), respectively] were used as references. The error bars represent ±s.d. (*n*=4 per group). Statistical significance was determined using Student's *t*-test with Welch's correction (**P*<0.05; ***P*<0.01; ****P*<0.001). D, dorsal; EP, electroporation; IHC, immunohistochemistry; L, lateral.

Dmrt factors inhibit neurogenesis in the medial telencephalon

The disorganization of the D-V boundary of the telencephalon is a striking phenotype in *Dmrt* DKO mutant embryos. However, Dmrt3 and Dmrta2 expression is actually much higher in the medial aspect of the telencephalon than dorsolaterally, suggesting that Dmrt3 and Dmrta2 may have additional roles in the medial cortex. Indeed, reports have demonstrated that *Dmrta2* single-mutant embryos exhibit a loss of the medial cortex, including the cortical hem, with milder abnormalities in D-V patterning (Fig. 2) (Konno et al., 2012; Saulnier et al., 2013). We next asked which step in the development of the medial telencephalon was dependent on Dmrt factors. To this end, we again performed acute loss-of-function experiments with Dmrt gene siRNAs in the medial telencephalon by *in utero* electroporation (Fig. 5A). Cells electroporated with siRNAs targeting *Dmrt3* and *Dmrta2* (DKD cells) at E11.5 largely differentiated into neurons and rapidly disappeared from the ventricular zone at E13.5, whereas the majority of cells with control siRNAs remained in the ventricular zone as Sox2-positive progenitors (Fig. 5B,C). In this assay, none of the ventral genes we examined exhibited significant changes in expression (Fig. S9A) (data not shown) in DKD cells, suggesting that Dmrt factors have a unique role in the medial telencephalon compared with their functions in the lateral telencephalon. We then asked which genes were affected by the loss of function of *Dmrt3* and *Dmrta2*. To this end, we performed transcriptomic analysis 24 h after electroporation, prior to the appearance of the neurogenic phenotype. Intriguingly, DKD cells exhibited the upregulation of dozens of genes (Fig. 5D). Among these upregulated genes, we focused on Pax6 given that it was expressed at the highest levels in our analysis and is an established promoter of neurogenesis. In DKD cells, *Pax6* expression was markedly elevated (2.1-fold) compared with control cells (Fig. 5E). Several genes encoding transcription factors, such as *Neurog2*, *Neurod1* and *Neurod6*, were also upregulated in DKD cells (Fig. 5E). These factors function directly or indirectly downstream of Pax6 (Sansom et al., 2009), consistent with the promotion of neurogenesis observed in DKD cells. Notably, both gene expression and histological analyses revealed that the additional knockdown of *Pax6* expression in DKD cells (TKD cells) rescued the neurogenic phenotype observed in DKD cells (Fig. 5F) (Fig. S9B-E). Taken together with the graded expression of Dmrt3 and Dmrta2 in the developing telencephalon, our observations suggest that Dmrt factors regulate region-dependent neurogenic properties of neural progenitors by establishing a lateral^{high}/medial^{low} gradient of Pax6 in the developing dorsal telencephalon.

Binding of Dmrt3 and Dmrta2 to *Gsx2* and *Pax6* enhancers

We next sought to identify Dmrt3- and Dmrta2-binding regions using whole-genome chromatin immunoprecipitation (ChIP)-sequencing and ChIP-qPCR analyses in tissue from the dorsal telencephalon of E12.5 mouse embryos. In these assays, we found that Dmrt3 and Dmrta2 bound to *Gsx2* and *Pax6* loci, and two binding regions were identified within ±100 kb from the transcription start site (TSS) of each locus (Fig. 6A-D). To

Development (2019) 146, dev174243. doi:10.1242/dev.174243

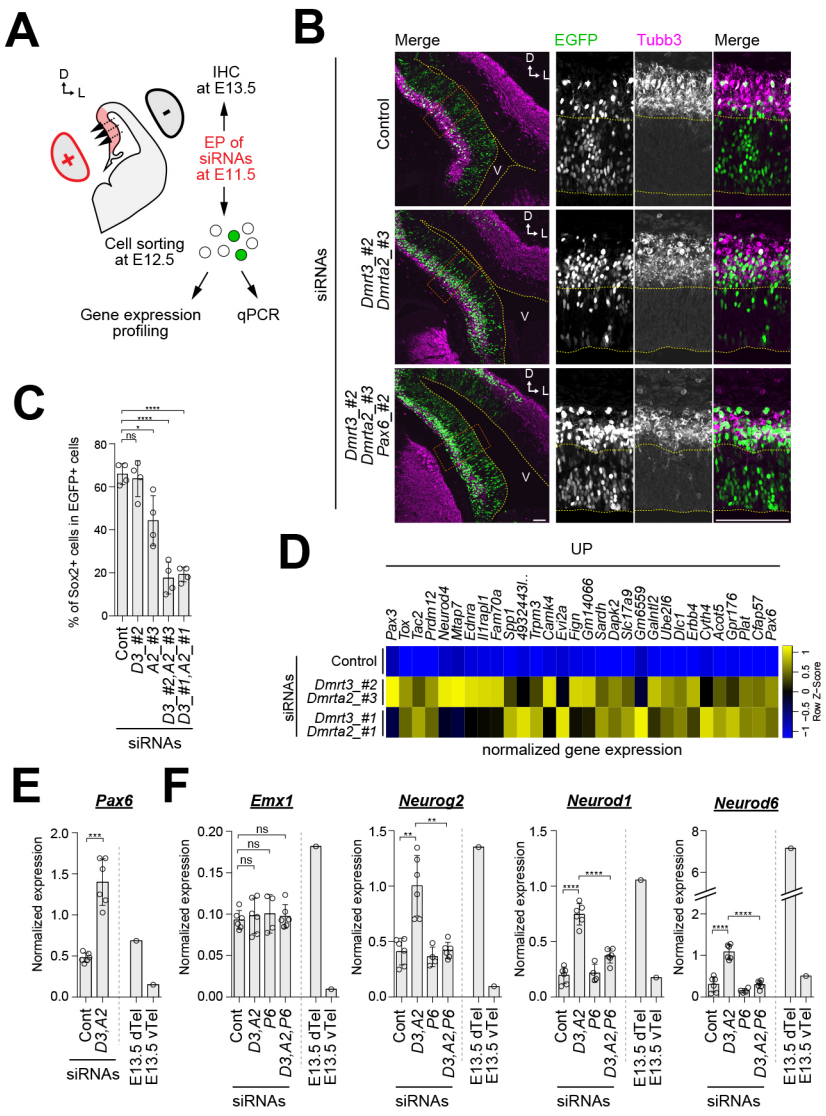

Fig. 5. Dmrt factors promote self-renewing ability in telencephalic progenitors. (A) Schematic summarizing the experimental design for histological (B,C) and gene expression (D) analyses in the medial telencephalon electroporated with siRNAs and the EGFP-NLS expression vector in the dorsolateral cortex at E11.5. (B) Immunofluorescence for Tubb3 and EGFP fluorescence in coronal sections of an E13.5 mouse telencephalon electroporated with control siRNAs (top) or siRNAs targeting *Dmrt3* and *Dmrta2* (middle), or siRNAs targeting *Dmrt3*, *Dmrta2* and *Pax6* (bottom). The yellow dotted lines indicate the ventricular surface. Scale bars: 100 µm. (C) The quantification of Sox2-positive neural progenitors in the electroporated cells at E13.5. The error bars represent ±s.d. (n=4 per group). (D) Transcriptome analysis of cells electroporated with two distinct sets of siRNAs targeting *Dmrt* (set1: *Dmrt3_#2* and *Dmrta2_#3*, set2: *Dmrt3_#1* and *Dmrta2_#1*) at E12.5. The heat-maps reflect normalized changes in gene expression that are upregulated following the knockdown of Dmrt genes. (E,F) Gene expression of *Pax6* (E), *Emx1* (F), *Neurog2* (F), *Neurod1* (F) and *Neurod6* (F) normalized to *Sox2* in the electroporated cells, as analyzed by qPCR. The error bars represent ±s.d. (n=6 per group in E and F). Statistical significance in C, E and F was determined using Student's t-test with Welch's correction (ns, not significant; $^{**}P$<0.01; $^{***}P$<0.001; $^{****}P$<0.0001). D, dorsal; EP, electroporation; IHC, immunohistochemistry; L, lateral.

determine the role of the sequences bound by Dmrt3 and Dmrta2, we performed ChIP-sequencing for histone modifications of histone H3 at lysines 4 and 27 using dorsal and ventral telencephalic samples from E12.5 wild-type mouse embryos. We found that Dmrt3- and Dmrta2-binding sites (DmrtBS) exhibited enrichment in lysine 4 monomethylation (H3K4me1) and lysine 27 acetylation (H3K27ac) on histone H3 (Fig. 6A,B). Given that nucleosomes in the vicinity of active enhancers typically contain both H3K4me1 and H3K27ac modifications (Shlyueva et al., 2014), we asked whether the Dmrt-binding sequences had enhancer activity for *Gsx2* or *Pax6* expression. To answer this, we generated transgenic mice in which EGFP expression was driven by the DmrtBS and *Hsp68* (*Hspa1*) minimal promoter (Fig. 6E,F). We observed EGFP expression in dLGE cells of transgenic mice harboring the DmrtBS located 6 kb downstream of the transcription termination site (TTS) of *Gsx2* (Fig. 6G). We also observed a lateral^{high}/medial^{low} EGFP expression gradient in dorsal telencephalic cells in transgenic mice harboring the DmrtBS located 22 kb downstream of the *Pax6* TTS site, which overlaps that of a reported *Pax6* forebrain enhancer (Fig. 6H) (McBride et al., 2011; Mi et al., 2013b). These results suggest that Dmrt factors may contribute to shaping of the *Gsx2* and *Pax6* expression domains by binding to their enhancer sequences.

Differential regulation of *Gsx2* and *Pax6* by Dmrt factors

Our results above show that *Pax6* and *Gsx2* expressions differentially respond to the expression levels of Dmrt factors. We next asked how *Gsx2* and *Pax6* gene expression is regulated by different doses of Dmrt factors. To address this question, *Dmrt* mutant ES cells were subjected to an *in vitro* differentiation protocol by which ES cells can be differentiated into the dorsal telencephalic cell fate with no addition of instructive growth factors (the SFEBq method) (Fig. 7A,B, Fig. S10A-C, Fig. S11A,B) (Eiraku et al., 2008). When *Dmrt* mutant ES cells were treated with smoothened agonist (SAG), which activates canonical Shh signaling, the expression levels of *Gsx2* and also *Dlx1* were induced in a dose-dependent manner (Fig. 7C). Notably, their expression was increased more efficiently in DKO and TKO cells compared with wild-type cells at the same concentration of SAG (Fig. 7C). By contrast, *Pax6* expression, which is negatively regulated by Shh signaling, was less sensitive to SAG treatment, and a much higher concentration was needed to reduce *Pax6* expression even in DKO and TKO cells (Fig. 7C). These results indicate that *Pax6* expression is robust against the weak Shh signaling that is sufficient to induce *Gsx2* expression in progenitors. Furthermore, consistent with the dose-dependent function of Dmrt factors *in vivo*, the concentration of SAG that is required to activate *Gsx2* expression was lower in

Development (2019) 146, dev174243. doi:10.1242/dev.174243

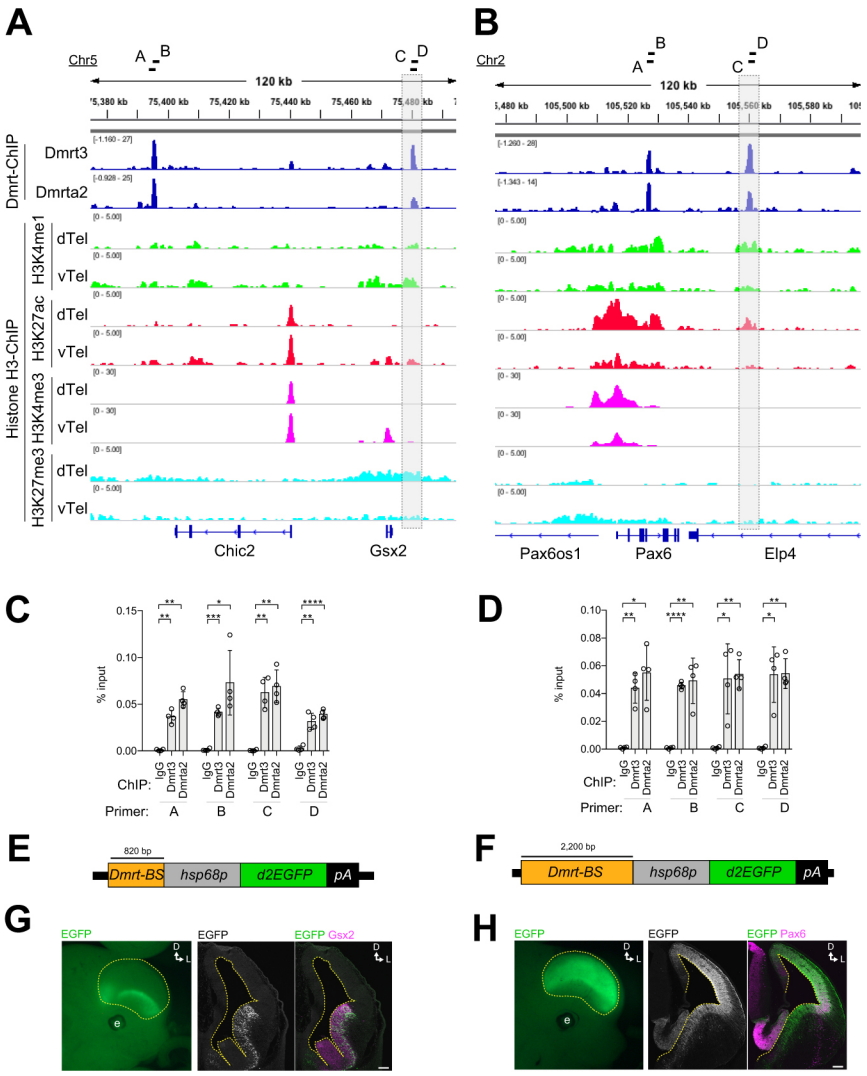

Fig. 6. Dmrt binds to the enhancer sequences of *Gsx2* and *Pax6*. (A,B) Distributions of ChIP-seq peaks obtained with antibodies for Dmrt3 (blue), Dmrta2 (blue), H3K4me1 (green), H3K4me3 (magenta), H3K27Ac (red), and H3K27me3 (light blue) at the *Gsx2* (A) and *Pax6* (B) loci in the E12.5 mouse telencephalon. The bars on the top with letters indicate the position of the primer sets used for ChIP-qPCR in C and D. (C,D) Quantification of Dmrt3/Dmrta2 binding at sequences within 100 kb from the *Gsx2* (C) and *Pax6* (D) TSSs, as determined by ChIP-qPCR. The error bars represent ±s.d. (n=4 per group). Statistical significance was determined using Student's t-test with Welch's correction (*P<0.05; **P<0.01; ***P<0.001; ****P<0.0001). (E,F) The structure of the transgene for visualizing enhancer activity of the Dmrt-binding site at the *Gsx2* (E) or the *Pax6* (F) locus. (G,H) Left: Lateral views of EGFP fluorescence of E12.5 transgenic mouse embryos generated by injecting the expression cassette indicated in E and F. Right: Immunostaining for Gsx2 (G) or Pax6 (H), with EGFP fluorescence, in coronal sections of the E12.5 telencephalon of transgenic mice E12.5. Scale bars: 100 µm. The yellow dotted lines indicate the outline of the telencephalon (right) and the ventricular surface (left).

TKO cells than that in DKO cells (Fig. 7C). When exogenous Dmrta2 was introduced by the Tet-On system (Fig. 7D,E), the expression of both *Gsx2* and *Pax6* was gradually and linearly decreased by step-wise increases of *Dmrta2* expression (Fig. 7F). The decrease in *Pax6* expression by Dmrta2 induction was much more attenuated than that of *Gsx2* (Fig. 7F), suggesting that Gsx2 expression is more sensitive to Dmrt factors than Pax6. Thus, the differential sensitivity of *Gsx2* and *Pax6* gene expression to Dmrt factors may explain the differential responses of these genes to manipulations of Dmrt levels.

Increased levels of Dmrt expands the cerebral cortical area

We lastly examined the effect of Dmrt factor overexpression *in vivo*. As described above, Dmrt factors (1) suppress the conversion of progenitor identity to dLGE fate by repressing *Gsx2* expression in the dorsolateral telencephalon and (2) maintain progenitors in a less neurogenic state by repressing *Pax6* in the medial telencephalon. We then speculated that the overexpression of Dmrt factors in progenitors would lead to a conversion of their division mode from more neurogenic to less neurogenic, resulting in expansion of the cerebral cortex. To test this hypothesis, we generated transgenic mice in which Flag-tagged Dmrt3 was overexpressed in neural progenitors using the nestin enhancer and the minimal thymidine kinase (*Tk*) gene promoter (Fig. 8A). The transgenic mice exhibited massive planar expansion of the ventricular surface, in association with marked reduction of the expression of Pax6 with no increase in ventral gene expression. This finding suggests that the division mode of telencephalic progenitors shifted to a more proliferative mode (Fig. 8B). Consistent with this conclusion, the number of cells expressing Tbr2, a transcription factor that positively regulates neuronal differentiation (Arnold et al., 2008; Sessa et al., 2008), was decreased in the transgenic mice compared with wild-type brains (Fig. 8C). We also found a subtle increase in the number of Tbr1-positive cells in mutants compared with wild-type embryos although this was not statistically significant (data not shown). Further study is needed to reveal the involvement of Dmrt factors in cortical layer formation. These findings imply that the graded expression of Dmrt factors along the D-V axis governs the proportional development of each brain region in the telencephalon and confers region-specific neurogenic properties to neural progenitors, consequently defining the pattern of the dorsal telencephalon.

DISCUSSION

Our findings describe a novel transcriptional network in which mammalian Dmrt factors orchestrate the development of the cerebral cortex. The medial^{high}/lateral^{low} gradient of Dmrt factor expression operates in two ways: (1) determination of the D-V

Development (2019) 146, dev174243. doi:10.1242/dev.174243

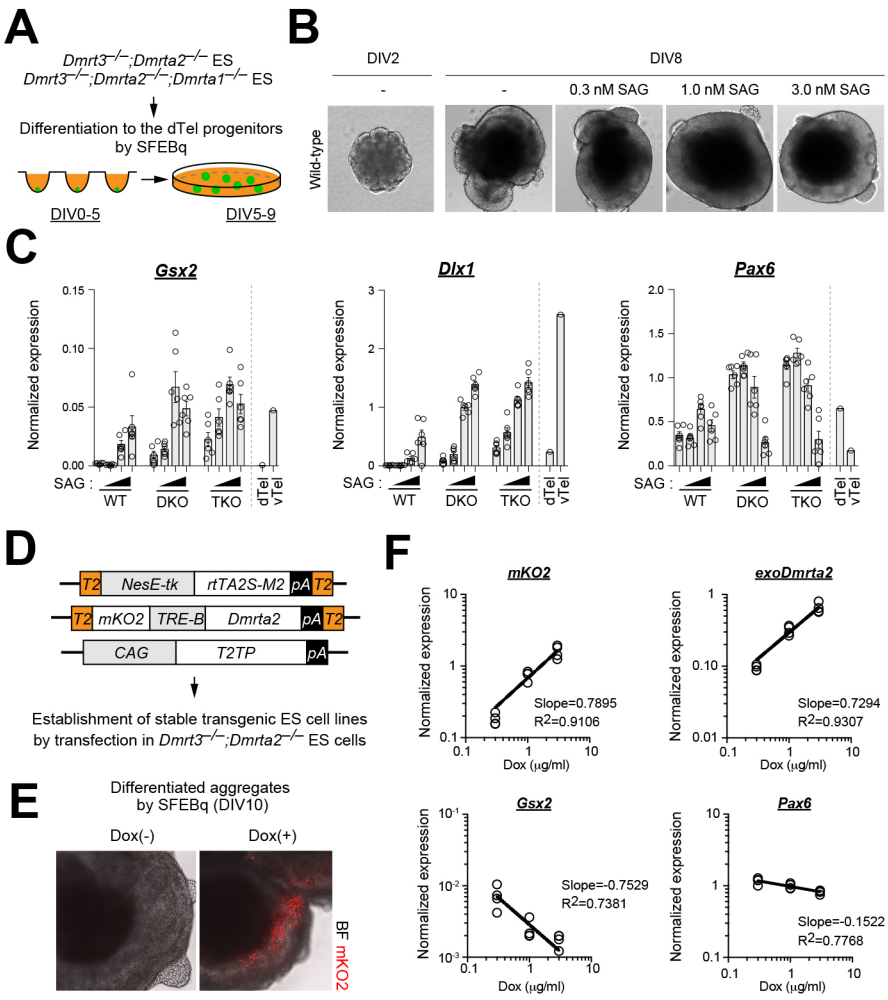

Fig. 7. Differential regulation of *Gsx2* and *Pax6* by Dmrt. (A) Schematic summarizing the formation of cerebral organoids from ES cells (SFEBq method). Control and mutant ES cells were differentiated into telencephalic (cerebral) progenitors *in vitro*. (B) Bright-field images of cerebral organoids established via the SFEBq method (day 2 and day 8) treated with or without SAG, a smoothened antagonist, at a concentration from 0 to 3.0 nM. (C) Gene expression of *Gsx2*, *Dlx1* and *Pax6* normalized to *Sox2* in organoids treated with SAG at the different concentrations (indicated in B) on day 9. The error bars represent ±s.e.m. (n=6 per group). (D) Schematic of the establishment of *Dmrt3*/*Dmrta2* double-knockout ES cells inducibly expressing *Dmrta2* under the control of the nestin enhancer and the Tet-ON system (TetON-Dmrta2). (E) mKO2 fluorescence induced with 1 μg/ml Dox from day 8 to day 10 in TetON-Dmrta2 cells differentiated by SFEBq. (F) Gene expression of *mKO2*, *exoDmrta2* (exogenously expressed *Dmrta2*), *Gsx2* and *Pax6* normalized to *Sox2* in SFEBq-differentiated TetON-Dmrta2 cells treated with Dox at concentrations from 0.3 to 3.0 μg/ml. n=4 per group. The solid lines represent a model fit obtained by non-linear regression analysis.

boundary by suppressing expression of the ventral gene *Gsx2*, a transcription factor essential for LGE and caudal ganglionic eminence cell fates; and (2) restriction of neurogenesis in the medial region through negative regulation of Pax6 expression.

Our results indicate that Dmrt factors repress *Gsx2* by binding to its enhancer, thereby determining the D-V boundary. A remaining question is the nature of the relationship between this Dmrt function and those of known patterning factors, such as Pax6 and Gli3, which have also been implicated in restriction of Gsx2 expression. Key findings in this regard come from previous studies analyzing the genetic interaction between Pax6 or Gli3, and Shh signaling. In the dorsal telencephalon of *Pax6* or *Gli3* mutant mice, *Gsx2* expression was shown to be ectopically increased, resulting in disorganization of the DV boundary (Toresson et al., 2000; Yun et al., 2001), similar to the phenotype seen in Dmrt mutant embryos. Intriguingly, additional knockout of the *Shh* gene in *Pax6* or *Gli3* mutants led to a partial rescue of this phenotype, indicating that the ventral restriction of *Gsx2* expression by Pax6 and Gli3 requires *Shh* function (Aoto et al., 2002; Fuccillo et al., 2006; Rallu et al., 2002; Rash and Grove, 2007). These results are consistent with reports that both Pax6 and Gli3 directly repress the expression of the *Shh* gene itself or that of Shh target genes, such as *Ptch1* (Caballero et al., 2014; Vokes et al., 2008). Taking these findings together with our results, it is likely that Dmrt factors repress *Gsx2* expression by direct binding to its enhancer independently of Shh function. In contrast, Pax6 and Gli3 likely repress *Gsx2* expression indirectly by suppressing Shh signaling and subsequently suppressing another downstream pathway, such as Fgf signaling. Consistent with this model, the additional knockout of the *Shh* gene in *Dmrt3* and *Dmrta2* DKO mice did not rescue the ectopic expression of *Gsx2*, and all neural progenitors located in the telencephalon of the triple-mutant embryos co-expressed both Pax6 and Gsx2 (data not shown). This result suggests that a ventralizing pathway other than Shh signaling positively regulates *Gsx2* expression. Remarkably, our *in vitro* experiments in which ES cells were differentiated to neural progenitors using cortical organoids showed that *Gsx2* expression did not change, or very slightly increased, in the absence of Shh agonist treatment, even in DKO and TKO cells. This result suggests that *Gsx2* expression *in vivo* is positively regulated indirectly by Shh or directly by unidentified exogenous factors (Fig. 8D).

Dmrt factors have different roles in medial telencephalic neural progenitors from those in the lateral telencephalon in developing mice. Our experiments using an acute loss-of-function system in the medial telencephalon showed that Dmrt factors maintain a less neurogenic state by reducing the expression of Pax6, which positively regulates neurogenic genes (Fig. 8D) (Sansom et al., 2009). On the other hand, Pax6 in the developing telencephalon negatively regulates cell cycle progression by directly suppressing the expression of cell cycle regulators, such as *Cdk6* (Mi et al., 2013a). In this manner, the graded expression pattern of Pax6 across the developing cortex leads to region-specific regulation of cell

Development (2019) 146, dev174243. doi:10.1242/dev.174243

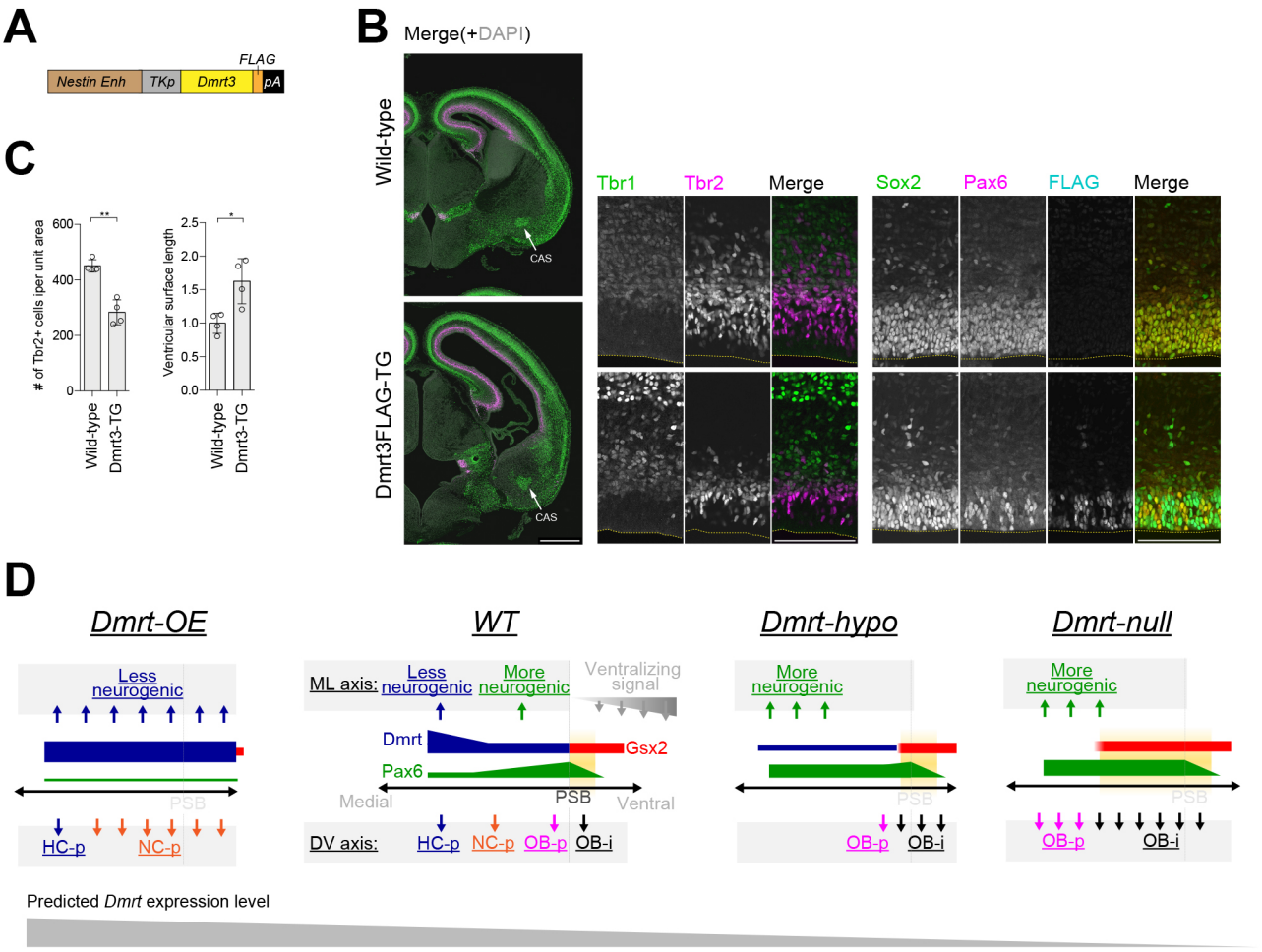

Fig. 8. Increased expression of Dmrt expands the cerebral cortical area. (A) Structure of the transgene for overexpressing FLAG-tagged Dmrt3 under the control of the nestin enhancer. (B) Immunofluorescence for Tbr1, Tbr2, Sox2 and Pax6 in coronal sections of wild-type and *Dmrt3-FLAG* transgenic mice at E15.5. The yellow dotted lines indicate the ventricular surface. Scale bars: 100 µm. CAS, caudal amygdaloid stream. (C) Quantification of Tbr2-positive basal progenitors in a unit area (left) and the relative length of the ventricular surface in the dorsal telencephalic area of transgenic animals (right). The error bars represent ±s.d. (n=4 per group). Statistical significance was determined using Student's t-test with Welch's correction (*P<0.05; **P<0.01). (D) Model illustrating the Dmrt transcriptional cascade and the production of cortical/subcortical neurons. Graded expression of Dmrt factors determines the positional information of cerebral cortical progenitors by differentially suppressing *Gsx2* and *Pax6*. HC-p, hippocampal projection neuron; hypo, hypoexpression; ML, medial-lateral; NC-p, neocortical projection neuron; OE, overexpression; WT, wild type.

cycle progression. Reports have shown that changing cell cycle length can alter the mode of cell division of neural progenitors in the developing cerebral cortex (Lange et al., 2009; Pilaz et al., 2009). Therefore, Dmrt factors may reduce the neurogenic potential of progenitors by repressing Pax6 activity and thereby shortening the cell cycle.

Our results showed that Dmrt factors negatively regulate the expression of two transcription factors, *Gsx2* and *Pax6*, in the developing dorsal telencephalon. These factors exhibit differential sensitivity to the dosage of Dmrt genes. In the case of *Gsx2*, a relatively lower amount of Dmrt factors can repress its expression in the dorsolateral telencephalon, whereas much higher Dmrt expression is required to suppress *Pax6* expression. Of particular interest, the differential response of *Gsx2* and *Pax6* expression to Dmrt factors permits a situation in which only *Pax6* but not *Gsx2* is expressed. In this way, graded neurogenic potential of neural progenitors across the developing cerebral cortex can be achieved and cortical glutamatergic neurons can be generated. The question arises of why *Gsx2* and *Pax6* are differentially sensitive to the same levels of Dmrt expression. The results of our *in vitro* differentiation experiments provide a clue in this regard. Increasing the expression of exogenous Dmrta2 in SFEBq-mediated neural differentiation induced a gradual decrease in the expression levels of both *Gsx2* and *Pax6*. However, the rate of decrease in the expression of *Gsx2* was higher than that of *Pax6* expression (Fig. 7F), suggesting at least three possibilities. First, Dmrt factors may have differential binding characteristics at *Gsx2* and *Pax6* enhancers. Second, the strength of the upstream pathways controlling *Gsx2* and *Pax6* expression might differ for these two genes. Third, differential regulation of histone modifications in these two enhancer regions may lead to the different response to the Dmrt binding. Indeed, suppressive H3K27me3 modification in the *Gsx2* enhancer appeared to be abundant compared with that in the *Pax6* enhancer in the dorsal telencephalon (Fig. 6A,B). Future studies to dissect the molecular properties of the Dmrt factors will likely reveal the mechanisms that underlie the differential dose dependence of Dmrt factors on the regulation of their target genes.

Recently, Desmaris et al. have reported a similar defect of dorsal-ventral patterning in *Dmrt3/Dmrt5* and *Emx2/Dmrt5* double mutants (Desmaris et al., 2018). This study is consistent with their previous report that Emx2 is a possible target of Dmrt5 (Saulnier et al., 2013). However, our study demonstrated that acute

Development (2019) 146, dev174243. doi:10.1242/dev.174243

knockdown of Dmrt3/Dmrta2 resulted in no significant changes in *Emx2* or *Emx1* (data not shown). We also confirmed that there was no binding of Dmrt3 and Dmrta2 on *Emx1* and *Emx2* gene loci by ChIP-seq analysis. This observation raises a possibility that the expression change of Emx1 and Emx2 observed in Dmrt mutants is a secondary effect of lacking the cortical hem, a primordium expressing multiple Wnt genes. Given that Emx2 is partly required for the formation of the cortical hem and the expression of Wnt genes (Tole et al., 2000a), we hypothesize that Dmrt factors interact with Wnt signaling to suppress the expression of Gsx2. Further study is needed to understand the precise molecular mechanisms for the interaction among Dmrt factors, Emx1/2, and Wnt signaling.

The degree of evolutionary conservation of Dmrt factor function in cortical development remains to be elucidated. Several reports have shown the specific expression of a few Dmrt 'A' family genes in the dorsal telencephalon of other vertebrate embryos, including chicken, *Xenopus* and zebrafish (Hong et al., 2007). Therefore, it seems likely that the essential role of Dmrt factors reported in the present manuscript is, at least in part, conserved across vertebrates. Taken together with our present findings regarding the crucial role of Dmrt factors in the developing dorsal telencephalon, we hypothesize that acquiring Dmrt expression might have been one of the key steps in the emergence of the cerebral cortex during evolution. This possibility is an intriguing question for future study.

MATERIALS AND METHODS

Animals

Embryonic stages were calculated by defining noon on the day of vaginal plug as E0.5. *Dmrt3* and *Dmrta2* mutant mice were maintained in a C57BL/6 background, as described previously (Konno et al., 2012). Genotyping of the *Dmrt3* allele was performed by PCR using the following primers: Dmrt3-P1: 5′-GGACCTGCGGGTGGAGCCTG-3′; Dmrt3-P2: 5′-GTCTGTCCTAGCTTCCTCACTG-3′; Dmrt3-P3: 5′-GATGAGGCTCTCCAGGCTCTCGTTG-3′. These primers yield bands of 462 and 336 bp for the wild-type and mutant alleles, respectively. Genotyping of *Dmrta2* alleles was performed by PCR using the following primers: Dmrta2-P1: 5′-ACTTCGGATCCTAGTGAACCTCTTCGAG-3′; Dmrta2-P2: 5′-TGCCTACGAAGTCTTTGGCTCGGTTTG-3′; Dmrta2-P3: 5′-TGGAGAGCCACAGTTAAGTAGTTGGAGC-3′. These primers yielded bands of 249 and 210 bp for the wild-type and mutant alleles, respectively. The generation of *Dmrta1* mutant mice was achieved by inducing a deletion in the vicinity of the initiation codon of *Dmrta1* using the CRISPR/Cas9 system, followed by injection of the mutant ES cells into 8-cell-stage mouse embryos (accession number CDB1303K, http://www2.clst.riken.jp/arg/mutant%20mice%20list.html) (see also Fig. S4D). Genotyping of *Dmrta1* alleles was performed by PCR using the following primers: Dmrta1-P1: 5′-TCCAGCCTGGCCCTTCTAGGCTC-3′; Dmrta1-P2: 5′-ACCGGAGCTTGCGGTCGATCGCAG-3′. These primers yielded bands of 450 and 350 bp for the wild-type and mutant alleles, respectively.

Dmrta2;Dmrt3-double heterozygotes exhibited normal fertility and CNS development. We therefore used these mice as controls in this study, except as noted.

All of the animal manipulations were performed according to the guidelines for animal experiments by Institutional Animal Care and Use Committee (IACUC) of RIKEN Kobe Branch.

Plasmids

pCAG-EGFP3NLS is an expression plasmid for 3xNLS-tagged EGFP and was described previously (Konno et al., 2008). pNesE-tk-rtTA2SM2 and pTRETi-mKO2_Dmrta2 are plasmids for the conditional expression of Dmrta2 and are based on the second generation of the Tet-On system (Tet-On Advanced, Invitrogen). pNesE-tk-rtTA2SM2 was constructed by inserting the enhancer sequence of the rat nestin gene (NesE) (Lothian and Lendahl, 1997) obtained using rat genomic DNA by PCR and inserted together with the thymidine kinase minimal promoter (tk) into the rtTA2SM2 expression plasmid (pTet-On Advanced, Clontech). pTRETi-mKO2_ Dmrta2 was constructed by inserting mKO2 [a red fluorescent protein (MBL, Nagoya, Japan)], and Dmrta2 amplified using E12.5 mouse forebrain cDNA by PCR into multiple cloning sites 1 and 2, respectively. The pNesE-tk-rtTA2SM2 and pTRETI-mKO2;Dmrta2 expression cassettes were then excised and inserted into pT2AL200R150G, in which the cloning site is flanked by the *Tol2* transposon elements (Urasaki et al., 2006). These elements then integrate into the genome in the presence of Tol2 transposase. pCAGGS-T2TP is a plasmid expressing the Tol2 transposase under the control of the CAG promoter (Kawakami and Noda, 2004). pPGK-PuroR is a plasmid expressing the puromycin-resistant gene (PuroR) under the control of the PGK promoter and was obtained from our animal facility (Laboratories of Animal Resource Development and Genetic Engineering, RIKEN CDB). pNesE-tk-Dmrt3-Flag is a plasmid for the transgenic expression of Flag-tagged Dmrt3 driven by the NesE-tk enhancer–promoter cassette. The plasmid was used to generate transgenic mice after removing the plasmid backbone by digesting with restriction enzymes.

In utero electroporation

In utero electroporation was performed at E11.5 as described previously (Fukuchi-Shimogori and Grove, 2001; Saito and Nakatsuji, 2001; Tabata and Nakajima, 2001). Briefly, CD-1 mouse embryos were electroporated with expression plasmids and siRNAs using an electroporator (CUY21, BEX, Tokyo, Japan) at the following concentrations: pCAG-EGFP3NLS, (0.5 μg/μl); siRNAs, 75 μM for *Dmrt3*, *Dmrta1* and *Pax6*; 150 μM for *Dmrta2*.

siRNAs

The following target sequences were used to synthesize the siRNAs (Invitrogen stealth siRNA) for knockdown experiments of mouse *Dmrt3*, *Dmrta2* and *Dmrta1*: *Dmrt3*_control (mutated *Dmrt3*_#2): 5′-GCGCGTTCGATAACCGATACACTGA-3′; *Dmrt3*_#1: 5′-TGAGGTCCCAGTATGTCAGTCCATT-3′; *Dmrt3*_#2: 5′-GCGCAGCTTGCTAAACCAGATCTGA-3′; *Dmrt3*_#3: 5′-GCCCTCTAGCGGCCATATCTTTGAA-3′; *Dmrta2*_control (mutated Dmrta2_#3): 5′-CAAGTACAGGATTGTTATCGTATTT-3′; *Dmrta2*_#1: 5′-GCCTACGAAGTCTTTGGCTCGGTTT-3′ *Dmrta2*_#2: 5′-GAAGGACTGCCTGTGCGCCAAGTGT-3′; *Dmrta2*_#3: 5′-CAAATTGCAGAAGTTTGATCTGTTT-3′; Dmrta1_control (mutated *Dmrta1*_#3): 5′-GGAAGACTTCAATCTATCACGGGTT-3′; *Dmrta1*_#1: 5′-GAGTGGGCCAGAGACTACATTGCTA-3′; *Dmrta1*_#2: 5′-CCACGAGACCCTCTCGGAATTCTTA-3′; *Dmrta1*_#3: 5′-GGAGGAGATTCAACTCTCTACAGTT-3′; *Pax6*_control (mutated in *Pax6*_#2): 5′-CCACGAACAAACCGTCCATTGTGCA-3′; *Pax6*_#1: 5′-ACCACACCTGTCTCCTCCTTCACAT-3′; *Pax6*_#2: 5′-CCATGGCAAACAACCTGCCTATGCA-3′; *Pax6*_#3: 5′-CATCAATAAACAGAGTTCTTCGCAA-3′. The knockdown efficiency of each siRNA was examined in HEK293 cells transfected with the siRNAs/expression plasmids at 24 h by western blotting. The transfections were performed using the Lipofectamine 2000 reagent (Invitrogen), according to the manufacturer's protocol.

Isolation of electroporated cells

Electroporated brain regions were dissected, incubated in 0.05% trypsin/HBSS(−) at 37°C for 10 min, and dissociated by adding 0.75% BSA/PBS(−) and pipetting gently. EGFP-positive transfected cells were collected using a SH800 cell sorter (Sony Corporation, Tokyo, Japan) with the ultra-purity mode. The cells were collected directly into TRIzol LS reagent (Invitrogen) and stored at −80°C until the purification of total RNA.

Establishment of ES cells

Knockout ES cells for *Dmrt3* and *Dmrta2* were established according to a previously described protocol (Kiyonari et al., 2010). Briefly, blastocysts obtained by crossing $Dmrt3^{+/-}$ and $Dmrta2^{flox/flox}$ mutant mice were cultured in iSTEM mouse ES cell media supplemented with 0.8 μM PD184352 (Stem Cell Sciences), 2 μM SU5402 (Stem Cell Sciences), 3 μM CHIR99021 (Stem Cell Sciences) and 1000 U/ml LIF (ESGRO) in feeder-free conditions. After hatching, the blastocyst inner cell masses were plated on mouse embryonic fibroblast (MEF) feeder cells, cultured for 5-7 days, trypsinized, and re-plated on MEF feeder cells. ES cell-like colonies were

Development (2019) 146, dev174243. doi:10.1242/dev.174243

picked and expanded 3-4 days after re-plating. After establishing *Dmrt3*$^{+/+}$;*Dmrta2*$^{flox/flox}$ or *Dmrt3*$^{-/-}$;*Dmrta2*$^{flox/flox}$ ES cells, the cells were transfected with a plasmid expressing Cre recombinase driven by polyoma enhancer/herpes simplex virus thymidine kinase (MC1) promoter to delete *Dmrta2* exon 2.

To establish the ES cell line that conditionally expresses Dmrta2 in *Dmrt3/Dmrta2* knockout ES cells, *Dmrt3*$^{-/-}$;*Dmrta2*$^{-/-}$ ES cells were transfected with pT2-NesEtk-rtTA2SM2, pT2-pTRETI-mKO2_Dmrta2, pCAGGS-T2TP, and pPGK-PuroR using the NEON Transfection System (Invitrogen), according to the manufacturer's protocol. Puromycin (2 µg/ml) was added at 24 h and removed 72 h after transfection to kill non-transfected cells. After recovering for a few days, individual colonies were picked and re-plated into two wells of a 96-well plate by equal splitting, allowing for the colony to expand and for checking transgene expression. The transgene expression was confirmed by the red fluorescence of mKO2 and by western blotting for Dmrta2 and mKO2 in SFEBq-differentiated ES cells treated with 1 µg/ml doxycycline (Dox) for 72 h from culture day 7.

To establish triple-mutant ES cells for *Dmrt3*, *Dmrta2* and *Dmrta1* (referred to as *Dmrt3*$^{-/-}$;*Dmrta2*$^{-/-}$;*Dmrta1*$^{-/-}$), the CRISPR/Cas9 system (Addgene) (Cong et al., 2013) was applied using the established ES cells. Briefly, *Dmrt3*$^{-/-}$;*Dmrta2*$^{-/-}$ ES cells were transfected with expression plasmids encoding SpCas9 and sgRNAs to delete the genomic sequence containing the start codon of *Dmrta1*. The isolation and expansion of ES cell clones were performed according to the procedures described above. The sgRNA target sequences and combinations for knocking out *Dmrta1* are described as follows: Set 1, 5′-GACCTAGGCGGGTCCTCAGC-3′ and 5′-GCGGGCTGCTGCGCCCGCTT-3′; Set 2, 5′-GACCTAGGCGGGT-CCTCAGC-3′ and 5′-GTCGGTGTCGTCGGGGATTC-3′. Homozygous deletion and the introduction of a frame-shift error in *Dmrta1* were confirmed by DNA sequencing.

cDNA synthesis

The appropriate amounts of tissue and cells were dissociated in TRIzol (for tissue samples) (Invitrogen) or TRIzol LS (for sorted cells) (Invitrogen) reagents. Total RNA was purified using a Qiagen RNeasy Mini kit with on-column DNaseI digestion (Qiagen). Approximately 100-500 ng of total RNA was used for the first-strand cDNA synthesis using SuperScript VILO cDNA Synthesis Kit (Invitrogen). All of the procedures were performed according to the manufacturer's protocols.

Real-time quantitative PCR

Real-time quantitative PCR (qPCR) was performed using Thermal Cycler Dice Real Time System TP860 (Takara Bio) with FastStart Universal SYBR Green Master Mix (Roche). For the RT-qPCR analysis, the Ct value was determined using the comparative Ct method (ΔΔCT method), and the expression level of target genes is reported as relative to that of *Sox2* or *Gapdh*. In ChIP-qPCR analysis, the amount of target DNA sequences was determined using the ΔΔCT method and reported as a percentage of that in the input sample in each experiment. The primer sequences used in RT-qPCR and ChIP-qPCR are listed in Table S1.

Microarray analysis

Cy3-labeled cRNA (1.65 µg) was fragmented at 60°C for 30 min in a reaction volume of 55 µl containing 25× fragmentation buffer and 10× blocking agent, following the manufacturer's instructions (Agilent). On completion of the fragmentation reaction, 55 µl of 2× GEx Hybridization Buffer HI-RPM was added to the fragmentation mixture and hybridized to Agilent Whole Mouse Genome Microarrays (G4846A) for 17 h at 65°C in a rotating Agilent hybridization oven. After hybridization, the microarrays were washed for 1 min at room temperature with GE Wash Buffer 1 (Agilent) and 1 min with 37°C GE Wash buffer 2 (Agilent). The slides were scanned immediately after washing on the Agilent DNA Microarray Scanner (G2505C) using the one-color scan setting for 4×44k array slides (scan area 61×21.6 mm, scan resolution 5 µm, dye channel set to green, green PMT set to 100%, NoXDR). The scanned images were analyzed with Feature Extraction Software 10.5.1.1 (Agilent) using default parameters (protocol GE1_105_Jan09 and Grid:026655_D_F_20100123) to obtain background-subtracted and spatially detrended Processed Signal intensities. The normalized signal intensities (log2 values) were calculated by Genespring Agilent GX11.0 software.

Immunohistochemistry

Immunohistochemistry was performed as described previously (Konno et al., 2012). Briefly, the brains were fixed in 1% paraformaldehyde in 0.1 M phosphate buffer (pH 7.4) at 4°C for 2 h. After preparing 12-µm-thick frozen coronal or sagittal sections of fixed brains using a cryostat (Leica), the sections were mounted on APS-coated slide glasses (Matsunami) and stained with the following antibodies: anti-Dmrt3 (rabbit, 1:5000) (Konno et al., 2012), anti-Dmrta2 (rabbit, 1:5000) (Konno et al., 2012), anti-Dmrta2 (rat, 1:2000) (Konno et al., 2012), anti-βIII-tubulin (mouse, 1:5000, clone Tuj1, Covance), anti-Gad2 (rabbit, 1:200, 3988, CST Japan), anti-Tbr1 (rabbit, 1:10,000, a gift from Dr. Robert Hevner, University of Washington), anti-Pou3f2 (Brn-2) (goat, 1:500, C-20, Santa Cruz Biotechnology), anti-Zbtb20 (rabbit, 1:500, HPA016815, Sigma-Aldrich), anti-Math2 (Neurod6) (goat, 1:500, L-15, Santa Cruz Biotechnology), anti-Dlx2 (guinea pig, 1:2000, a gift from Dr. Kazuaki Yoshikawa, Osaka University), anti-Gsh2 (Gsx2) (rabbit, 1:10,000, a gift from Dr. Yoshiki Sasai, RIKEN CDB), anti-Pax6 (rabbit, 1:500, PRB-278P, Covance), anti-Sp8 (goat, 1:1000, C-18, Santa Cruz Biotechnology), anti-Isl1 (mouse, 1:20, Developmental Studies Hybridoma Bank), anti-Er81 (rabbit, 1:20, a gift from Dr Silvia Arber, University of Basel), anti-Sox2 (goat, 1:1000, Y-17, Santa Cruz Biotechnology), anti-Sox2 (rat, 1:1000, clone Btjce, eBioscience), anti-calretinin (goat, 1:200, AF5065, R&D Systems), anti-tyrosine hydroxylase (TH) (rabbit, 1:200, AB152, EMD Millipore), anti-Eomes (Tbr2) (rat, 1:1000, clone Dan11mag, eBioscience), anti-DYKDDDDKtag (Flag) (mouse, 1:1000, clone 1E6, Wako Pure Chemical Industries), anti-Emx1 [1:10,000, clone 1H8B11, a monoclonal antibody generated by immunizing a synthetic peptide (CKQANGEDIDVTSND) in rats, Cell Engineering Corporation, Osaka, Japan], anti-Neurog2 (goat, 1:200, C-16, Santa Cruz Biotechnology), anti-hAsc1 (Ascl1) (mouse, 1:1000, clone 24B72D11.1, BD-Japan), anti-ASH1 (Ascl1) (rabbit 1:1000, SK-T01-003, Cosmo Bio), anti-Bf1 (Foxg1) (goat, 1:200, N-15, Santa Cruz Biotechnology), anti-Bf1 (Foxg1) (rabbit, 1:500, M227, Takara Bio), anti-Lhx2 (goat, 1:500, C-20, Santa Cruz Biotechnology) and anti-Lmx1a (rabbit, 1:2000, AB10533, EMD Millipore). The primary antibodies were visualized with the secondary antibodies conjugated to Alexa 488, Cy3 and Cy5 (donkey, 1:500, 715-545-151, 715-165-151, 715-605-151, 711-545-152, 711-165-152, 711-605-152, 712-545-153, 712-165-153, 712-605-153, 706-545-148, 706-165-148, 706-605-148, 705-545-147, 705-165-147, 705-605-147, Jackson ImmunoResearch). For staining with mouse monoclonal antibodies, the sections were pre-incubated with monovalent Fab fragments (Jackson ImmunoResearch) to reduce the background signals on the mouse tissues. Apoptotic cells were detected by TUNEL (terminal deoxynucleotidyl transferase dUTP nick-end labeling) staining using the In Situ Cell Death Detection kit (Roche Diagnostics). All of the fluorescent images were acquired using Olympus FV1000 confocal microscope (Olympus).

Chromatin immunoprecipitation (ChIP)

The E12.5 wild-type CD-1 forebrain samples were fixed in D-PBS(−) containing 0.5% paraformaldehyde at room temperature for 5 min. After washing with ice-cold D-PBS(−) containing 0.1 M glycine twice, the brains were dissociated in ChIP buffer [10 mM Tris-HCl (pH 8.0), 200 mM KCl, 1 mM $CaCl_2$, 0.5% NP40] containing protease inhibitor cocktail (EDTA free) (25955-11, Nacalai Tesque) with a pestle homogenizer and briefly sonicated (Handy Sonic UR-20P, Tomy Seiko Co.). After sonication, the suspension was treated with 50 units/ml micrococcal nuclease (Worthington Biochemical) for 60 min at 37°C, with mild agitation for every 10 min. The nuclease reaction was stopped by adding ethylenediaminetetraacetic acid (EDTA; final concentration of 10 mM). After briefly sonicating again and centrifuging at 15,000 ***g*** for 10 min at 4°C, the supernatant was collected. The supernatants were then incubated at 4°C for 1 h with anti-mouse or anti-rabbit IgG magnetic beads (Dynabeads, Life Technologies) pre-bound with the following antibodies (2 µg antibody/20 µl Dynabeads suspension): rabbit normal IgG (Jackson ImmunoResearch), rabbit anti-Dmrt3 (Konno et al., 2012), rabbit anti-Dmrta2 (Konno et al., 2012), mouse anti-HistoneH3K4me (Ab8895, Abcam), mouse anti-HistoneH3K4me3,

Development (2019) 146, dev174243. doi:10.1242/dev.174243

mouse anti-HistoneH3K27ac (Ab4729, Abcam), or mouse anti-HistoneH3K27me3 (Kimura et al., 2008). The beads were briefly washed three times with ChIP buffer and three times with ChIP wash buffer [10 mM Tris-HCl (pH 8.0), 500 mM KCl, 1 mM CaCl2, 0.5% NP40]. The beads were treated in elution buffer [50 mM Tris-HCl (pH 8.0), 10 mM EDTA, and 1% sodium dodecyl sulfate] containing 20 µg/ml RNase (Sigma-Aldrich) at 37°C for 10 min and eluted by adding 20 µg/ml Proteinase K (Roche Diagnostics) and incubated at 55°C for 16 h. The DNA was recovered using a DNA gel extraction kit (Promega) and used for ChIP-qPCR analysis and ChIP-seq analysis.

Transgenic mice

Transgenic mice were generated by injecting the linearized expression cassettes derived from pNesEtk-Dmrt3-Flag into fertilized oocytes derived from CD-1 mouse strains. All of the transgenic animals were analyzed in transgenic founder (F0) embryos at E15.5.

RNA-sequencing

The RNA-seq libraries were prepared using TruSeq RNA Sample Preparation v2 kit and sequenced using an Illumina Genome analyzer-II X. The expression levels of genes were estimated using Cufflinks (version 2.2.1, options 'cuffdiff –u –b') with reads mapped onto the mouse genome (mm9) using TopHat (version 2.0.12) with default parameters.

ChIP-sequencing

The ChIP library was prepared using NEBNext Ultra DNA Library Prep kit for Illumina (New England Biolabs) and sequenced on the Illumina HiSeq1500 system (Illumina). The sequenced reads of ChIP and input DNA controls were mapped to the mouse genome (mm9) using bowtie2 with default parameters (version 2.2.3) (Langmead and Salzberg, 2012). The multi-reads were discarded by filtering 'XS:I' tags, and PCR-duplicate reads were discarded using SAMtools (Li et al., 2009). The mapped reads were counted in non-overlapping 100 base windows, and the counts were normalized as reads per million (RPM). We then calculated the normalized ChIP-Seq signal intensities on each window as RPM difference between ChIP and input DNA control data (i.e. RPM_{ChIP}–RPM_{Input}).

Quantifications

All of the statistical analyses were performed with Student's *t*-test with Welch's correction or one-way ANOVA using Prism 6 or R. The data were expressed as the mean±s.d. or ±s.e.m., as indicated in figure legends. Across all experiments, the data distribution was assumed to be normal, although the normality was not formally tested.

Gene ontology (GO) analysis

GO enrichment analysis was performed using PANTHER Classification System (Mi et al., 2013c) on the Gene Ontology Consortium website (http://geneontology.org).

Acknowledgements

We thank Matsuzaki laboratory members for helpful discussions and the animal resource facility members of RIKEN BDR for producing and maintaining the mutant mice.

Competing interests

The authors declare no competing or financial interests.

Author contributions

Conceptualization: D.K., F.M.; Methodology: D.K.; Software: D.K.; Validation: D.K.; Formal analysis: D.K.; Investigation: D.K., C.K., K.M., Y.O., H.K., S.O.; Resources: D.K., H.K.; Data curation: D.K.; Writing - original draft: D.K.; Writing - review & editing: D.K., F.M.; Visualization: D.K.; Supervision: D.K., F.M.; Project administration: D.K., F.M.; Funding acquisition: D.K.

Funding

This work was supported by Ministry of Education, Culture, Sports, Science and Technology/Japan Society for the Promotion of Science KAKENHI grants (JP22700361, JP24500395, JP25123724, JP15K06727, JP19H05266, JP18H05527).

Data availability

Microarray data and NGS data have been deposited in Gene Expression Omnibus under accession number GSE83639 and in the DNA Data Bank of Japan under accession number DRA004335.

Supplementary information

Supplementary information available online at http://dev.biologists.org/lookup/doi/10.1242/dev.174243.supplemental

References

Anderson, S., Mione, M., Yun, K. and Rubenstein, J. L. R. (1999). Differential origins of neocortical projection and local circuit neurons: role of Dlx genes in neocortical interneuronogenesis. *Cereb. Cortex* **9**, 646-654. doi:10.1093/cercor/9.6.646

Aoto, K., Nishimura, T., Eto, K. and Motoyama, J. (2002). Mouse GLI3 regulates Fgf8 expression and apoptosis in the developing neural tube, face, and limb bud. *Dev. Biol.* **251**, 320-332. doi:10.1006/dbio.2002.0811

Arnold, S. J., Huang, G.-J., Cheung, A. F. P., Era, T., Nishikawa, S.-I., Bikoff, E. K., Molnár, Z., Robertson, E. J. and Groszer, M. (2008). The T-box transcription factor Eomes/Tbr2 regulates neurogenesis in the cortical subventricular zone. *Genes Dev.* **22**, 2479-2484. doi:10.1101/gad.475408

Caballero, I. M., Manuel, M. N., Molinek, M., Quintana-Urzainqui, I., Mi, D., Shimogori, T. and Price, D. J. (2014). Cell-autonomous repression of Shh by transcription factor Pax6 regulates diencephalic patterning by controlling the central diencephalic organizer. *Cell Rep.* **8**, 1405-1418. doi:10.1016/j.celrep.2014.07.051

Ceci, M. L., Pedraza, M. and de Carlos, J. A. (2012). The embryonic septum and ventral pallium, new sources of olfactory cortex cells. *PLoS ONE* **7**, e44716. doi:10.1371/journal.pone.0044716

Cong, L., Ran, F. A., Cox, D., Lin, S., Barretto, R., Habib, N., Hsu, P. D., Wu, X., Jiang, W., Marraffini, L. A. et al. (2013). Multiplex genome engineering using CRISPR/Cas systems. *Science* **339**, 819-823. doi:10.1126/science.1231143

Corbin, J. G., Rutlin, M., Gaiano, N. and Fishell, G. (2003). Combinatorial function of the homeodomain proteins Nkx2.1 and Gsh2 in ventral telencephalic patterning. *Development* **130**, 4895-4906. doi:10.1242/dev.00717

Dave, R. K., Ellis, T., Toumpas, M. C., Robson, J. P., Julian, E., Adolphe, C., Bartlett, P. F., Cooper, H. M., Reynolds, B. A. and Wainwright, B. J. (2011). Sonic hedgehog and notch signaling can cooperate to regulate neurogenic divisions of neocortical progenitors. *PLoS ONE* **6**, e14680. doi:10.1371/journal.pone.0014680

Desmaris, E., Keruzore, M., Saulnier, A., Ratié, L., Assimacopoulos, S., De Clercq, S., Nan, X., Roychoudhury, K., Qin, S., Kricha, S. et al. (2018). DMRT5, DMRT3 and EMX2 cooperatively repress Gsx2 at the pallium-subpallium boundary to maintain cortical identity in dorsal telencephalic progenitors. *J. Neurosci.* **38**, 9105-9121. doi:10.1523/JNEUROSCI.0375-18.2018

Dessaud, E., McMahon, A. P. and Briscoe, J. (2008). Pattern formation in the vertebrate neural tube: a sonic hedgehog morphogen-regulated transcriptional network. *Development* **135**, 2489-2503. doi:10.1242/dev.009324

Ehrman, L. A., Mu, X., Waclaw, R. R., Yoshida, Y., Vorhees, C. V., Klein, W. H. and Campbell, K. (2013). The LIM homeobox gene Isl1 is required for the correct development of the striatonigral pathway in the mouse. *Proc. Natl. Acad. Sci. USA* **110**, E4026-E4035. doi:10.1073/pnas.1308275110

Eiraku, M., Watanabe, K., Matsuo-Takasaki, M., Kawada, M., Yonemura, S., Matsumura, M., Wataya, T., Nishiyama, A., Muguruma, K. and Sasai, Y. (2008). Self-organized formation of polarized cortical tissues from ESCs and its active manipulation by extrinsic signals. *Cell Stem Cell* **3**, 519-532. doi:10.1016/j.stem.2008.09.002

Fuccillo, M., Rutlin, M. and Fishell, G. (2006). Removal of Pax6 partially rescues the loss of ventral structures in Shh null mice. *Cereb. Cortex* **16** Suppl. 1, i96-i102. doi:10.1093/cercor/bhk023

Fukuchi-Shimogori, T. and Grove, E. A. (2001). Neocortex patterning by the secreted signaling molecule FGF8. *Science* **294**, 1071-1074. doi:10.1126/science.1064252

Grove, E. A., Tole, S., Limon, J., Yip, L. and Ragsdale, C. W. (1998). The hem of the embryonic cerebral cortex is defined by the expression of multiple Wnt genes and is compromised in Gli3-deficient mice. *Development* **125**, 2315-2325.

Hébert, J. M. and Fishell, G. (2008). The genetics of early telencephalon patterning: some assembly required. *Nat. Rev. Neurosci.* **9**, 678-685. doi:10.1038/nrn2463

Hoch, R. V., Rubenstein, J. L. R. and Pleasure, S. (2009). Genes and signaling events that establish regional patterning of the mammalian forebrain. *Semin. Cell Dev. Biol.* **20**, 378-386. doi:10.1016/j.semcdb.2009.02.005

Hong, C.-S., Park, B.-Y. and Saint-Jeannet, J.-P. (2007). The function of Dmrt genes in vertebrate development: It is not just about sex. *Dev. Biol.* **310**, 1-9. doi:10.1016/j.ydbio.2007.07.035

Kawakami, K. and Noda, T. (2004). Transposition of the Tol2 element, an Ac-like element from the Japanese medaka fish Oryzias latipes, in mouse embryonic stem cells. *Genetics* **166**, 895-899. doi:10.1534/genetics.166.2.895

Kimura, H., Hayashi-Takanaka, Y., Goto, Y., Takizawa, N. and Nozaki, N. (2008). The organization of histone H3 modifications as revealed by a panel of specific monoclonal antibodies. *Cell Struct. Funct.* **33**, 61-73. doi:10.1247/csf.07035

Kiyonari, H., Kaneko, M., Abe, S.-I. and Aizawa, S. (2010). Three inhibitors of FGF receptor, ERK, and GSK3 establishes germline-competent embryonic stem cells of C57BL/6N mouse strain with high efficiency and stability. *Genesis* **48**, 317-327. doi:10.1002/dvg.20614

Konno, D., Shioi, G., Shitamukai, A., Mori, A., Kiyonari, H., Miyata, T. and Matsuzaki, F. (2008). Neuroepithelial progenitors undergo LGN-dependent planar divisions to maintain self-renewability during mammalian neurogenesis. *Nat. Cell Biol.* **10**, 93-101. doi:10.1038/ncb1673

Konno, D., Iwashita, M., Satoh, Y., Momiyama, A., Abe, T., Kiyonari, H. and Matsuzaki, F. (2012). The mammalian DM domain transcription factor Dmrta2 is required for early embryonic development of the cerebral cortex. *PLoS ONE* **7**, e46577. doi:10.1371/journal.pone.0046577

Kroll, T. T. and O'Leary, D. D. M. (2005). Ventralized dorsal telencephalic progenitors in Pax6 mutant mice generate GABA interneurons of a lateral ganglionic eminence fate. *Proc. Natl. Acad. Sci. U.S.A.* **102**, 7374-7379. doi:10.1073/pnas.0500819102

Kuschel, S., Rüther, U. and Theil, T. (2003). A disrupted balance between Bmp/Wnt and Fgf signaling underlies the ventralization of the Gli3 mutant telencephalon. *Dev. Biol.* **260**, 484-495. doi:10.1016/S0012-1606(03)00252-5

Lange, C., Huttner, W. B. and Calegari, F. (2009). Cdk4/cyclinD1 overexpression in neural stem cells shortens G1, delays neurogenesis, and promotes the generation and expansion of basal progenitors. *Cell Stem Cell* **5**, 320-331. doi:10.1016/j.stem.2009.05.026

Langmead, B. and Salzberg, S. L. (2012). Fast gapped-read alignment with Bowtie 2. *Nat. Methods* **9**, 357-359. doi:10.1038/nmeth.1923

Li, H., Handsaker, B., Wysoker, A., Fennell, T., Ruan, J., Homer, N., Marth, G., Abecasis, G., Durbin, R. and 1000 Genome Project Data Processing Subgroup. (2009). The sequence alignment/Map format and SAMtools. *Bioinformatics* **25**, 2078-2079. doi:10.1093/bioinformatics/btp352

Long, J. E., Cobos, I., Potter, G. B. and Rubenstein, J. L. R. (2009). Dlx1&2 and Mash1 transcription factors control MGE and CGE patterning and differentiation through parallel and overlapping pathways. *Cereb. Cortex* **19** Suppl. 1, i96-i106. doi:10.1093/cercor/bhp045

Lothian, C. and Lendahl, U. (1997). An evolutionarily conserved region in the second intron of the human nestin gene directs gene expression to CNS progenitor cells and to early neural crest cells. *Eur. J. Neurosci.* **9**, 452-462. doi:10.1111/j.1460-9568.1997.tb01622.x

Martynoga, B., Drechsel, D. and Guillemot, F. (2012). Molecular control of neurogenesis: a view from the mammalian cerebral cortex. *Cold Spring Harb. Perspect. Biol.* **4**, a008359. doi:10.1101/cshperspect.a008359

McBride, D. J., Buckle, A., van Heyningen, V. and Kleinjan, D. A. (2011). DNaseI hypersensitivity and ultraconservation reveal novel, interdependent long-range enhancers at the complex Pax6 cis-regulatory region. *PLoS ONE* **6**, e28616. doi:10.1371/journal.pone.0028616

Mi, D., Carr, C. B., Georgala, P. A., Huang, Y.-T., Manuel, M. N., Jeanes, E., Niisato, E., Sansom, S. N., Livesey, F. J., Theil, T. et al. (2013a). Pax6 exerts regional control of cortical progenitor proliferation via direct repression of Cdk6 and hypophosphorylation of pRb. *Neuron* **78**, 269-284. doi:10.1016/j.neuron.2013.02.012

Mi, D., Huang, Y.-T., Kleinjan, D. A., Mason, J. O. and Price, D. J. (2013b). Identification of genomic regions regulating Pax6 expression in embryonic forebrain using YAC reporter transgenic mouse lines. *PLoS ONE* **8**, e80208. doi:10.1371/journal.pone.0080208

Mi, H., Muruganujan, A., Casagrande, J. T. and Thomas, P. D. (2013c). Large-scale gene function analysis with the PANTHER classification system. *Nat. Protoc.* **8**, 1551-1566. doi:10.1038/nprot.2013.092

Paridaen, J. T. M. L. and Huttner, W. B. (2014). Neurogenesis during development of the vertebrate central nervous system. *EMBO Rep.* **15**, 351-364. doi:10.1002/embr.201438447

Pilaz, L.-J., Patti, D., Marcy, G., Ollier, E., Pfister, S., Douglas, R. J., Betizeau, M., Gautier, E., Cortay, V., Doerflinger, N. et al. (2009). Forced G1-phase reduction alters mode of division, neuron number, and laminar phenotype in the cerebral cortex. *Proc. Natl. Acad. Sci. USA* **106**, 21924-21929. doi:10.1073/pnas.0909894106

Rallu, M., Machold, R., Gaiano, N., Corbin, J. G., McMahon, A. P. and Fishell, G. (2002). Dorsoventral patterning is established in the telencephalon of mutants lacking both Gli3 and Hedgehog signaling. *Development* **129**, 4963-4974.

Rash, B. G. and Grove, E. A. (2007). Patterning the dorsal telencephalon: a role for sonic hedgehog? *J. Neurosci.* **27**, 11595-11603. doi:10.1523/JNEUROSCI.3204-07.2007

Saito, T. and Nakatsuji, N. (2001). Efficient gene transfer into the embryonic mouse brain using in vivo electroporation. *Dev. Biol.* **240**, 237-246. doi:10.1006/dbio.2001.0439

Sansom, S. N., Griffiths, D. S., Faedo, A., Kleinjan, D.-J., Ruan, Y., Smith, J., van Heyningen, V., Rubenstein, J. L. and Livesey, F. J. (2009). The level of the transcription factor Pax6 is essential for controlling the balance between neural stem cell self-renewal and neurogenesis. *PLoS Genet.* **5**, e1000511. doi:10.1371/journal.pgen.1000511

Saulnier, A., Keruzore, M., De Clercq, S., Bar, I., Moers, V., Magnani, D., Walcher, T., Filippis, C., Kricha, S., Parlier, D. et al. (2013). The doublesex homolog Dmrt5 is required for the development of the caudomedial cerebral cortex in mammals. *Cereb. Cortex* **23**, 2552-2567. doi:10.1093/cercor/bhs234

Sessa, A., Mao, C.-A., Hadjantonakis, A.-K., Klein, W. H. and Broccoli, V. (2008). Tbr2 directs conversion of radial glia into basal precursors and guides neuronal amplification by indirect neurogenesis in the developing neocortex. *Neuron* **60**, 56-69. doi:10.1016/j.neuron.2008.09.028

Shlyueva, D., Stampfel, G. and Stark, A. (2014). Transcriptional enhancers: from properties to genome-wide predictions. *Nat. Rev. Genet.* **15**, 272-286. doi:10.1038/nrg3682

Stoykova, A., Treichel, D., Hallonet, M. and Gruss, P. (2000). Pax6 modulates the dorsoventral patterning of the mammalian telencephalon. *J. Neurosci.* **20**, 8042-8050. doi:10.1523/JNEUROSCI.20-21-08042.2000

Tabata, H. and Nakajima, K. (2001). Efficient in utero gene transfer system to the developing mouse brain using electroporation: visualization of neuronal migration in the developing cortex. *Neuroscience* **103**, 865-872. doi:10.1016/S0306-4522(01)00016-1

Theil, T., Alvarez-Bolado, G., Walter, A. and Rüther, U. (1999). Gli3 is required for Emx gene expression during dorsal telencephalon development. *Development* **126**, 3561-3571.

Tole, S., Goudreau, G., Assimacopoulos, S. and Grove, E. A. (2000a). Emx2 is required for growth of the hippocampus but not for hippocampal field specification. *J. Neurosci.* **20**, 2618-2625. doi:10.1523/JNEUROSCI.20-07-02618.2000

Tole, S., Ragsdale, C. W. and Grove, E. A. (2000b). Dorsoventral patterning of the telencephalon is disrupted in the mouse mutant extra-toes(J). *Dev. Biol.* **217**, 254-265. doi:10.1006/dbio.1999.9509

Toresson, H., Potter, S. S. and Campbell, K. (2000). Genetic control of dorsal-ventral identity in the telencephalon: opposing roles for Pax6 and Gsh2. *Development* **127**, 4361-4371.

Urasaki, A., Morvan, G. and Kawakami, K. (2006). Functional dissection of the Tol2 transposable element identified the minimal cis-sequence and a highly repetitive sequence in the subterminal region essential for transposition. *Genetics* **174**, 639-649. doi:10.1534/genetics.106.060244

Vokes, S. A., Ji, H., Wong, W. H. and McMahon, A. P. (2008). A genome-scale analysis of the cis-regulatory circuitry underlying sonic hedgehog-mediated patterning of the mammalian limb. *Genes Dev.* **22**, 2651-2663. doi:10.1101/gad.1693008

Waclaw, R. R., Allen, Z. J., Bell, S. M., Erdélyi, F., Szabó, G., Potter, S. S. and Campbell, K. (2006). The zinc finger transcription factor Sp8 regulates the generation and diversity of olfactory bulb interneurons. *Neuron* **49**, 503-516. doi:10.1016/j.neuron.2006.01.018

Wang, B., Long, J. E., Flandin, P., Pla, R., Waclaw, R. R., Campbell, K. and Rubenstein, J. L. R. (2013). Loss of Gsx1 and Gsx2 function rescues distinct phenotypes in Dlx1/2 mutants. *J. Comp. Neurol.* **521**, 1561-1584. doi:10.1002/cne.23242

Wichterle, H., Garcia-Verdugo, J. M., Herrera, D. G. and Alvarez-Buylla, A. (1999). Young neurons from medial ganglionic eminence disperse in adult and embryonic brain. *Nat. Neurosci.* **2**, 461-466. doi:10.1038/8131

Yun, K., Potter, S. and Rubenstein, J. L. (2001). Gsh2 and Pax6 play complementary roles in dorsoventral patterning of the mammalian telencephalon. *Development* **128**, 193-205.

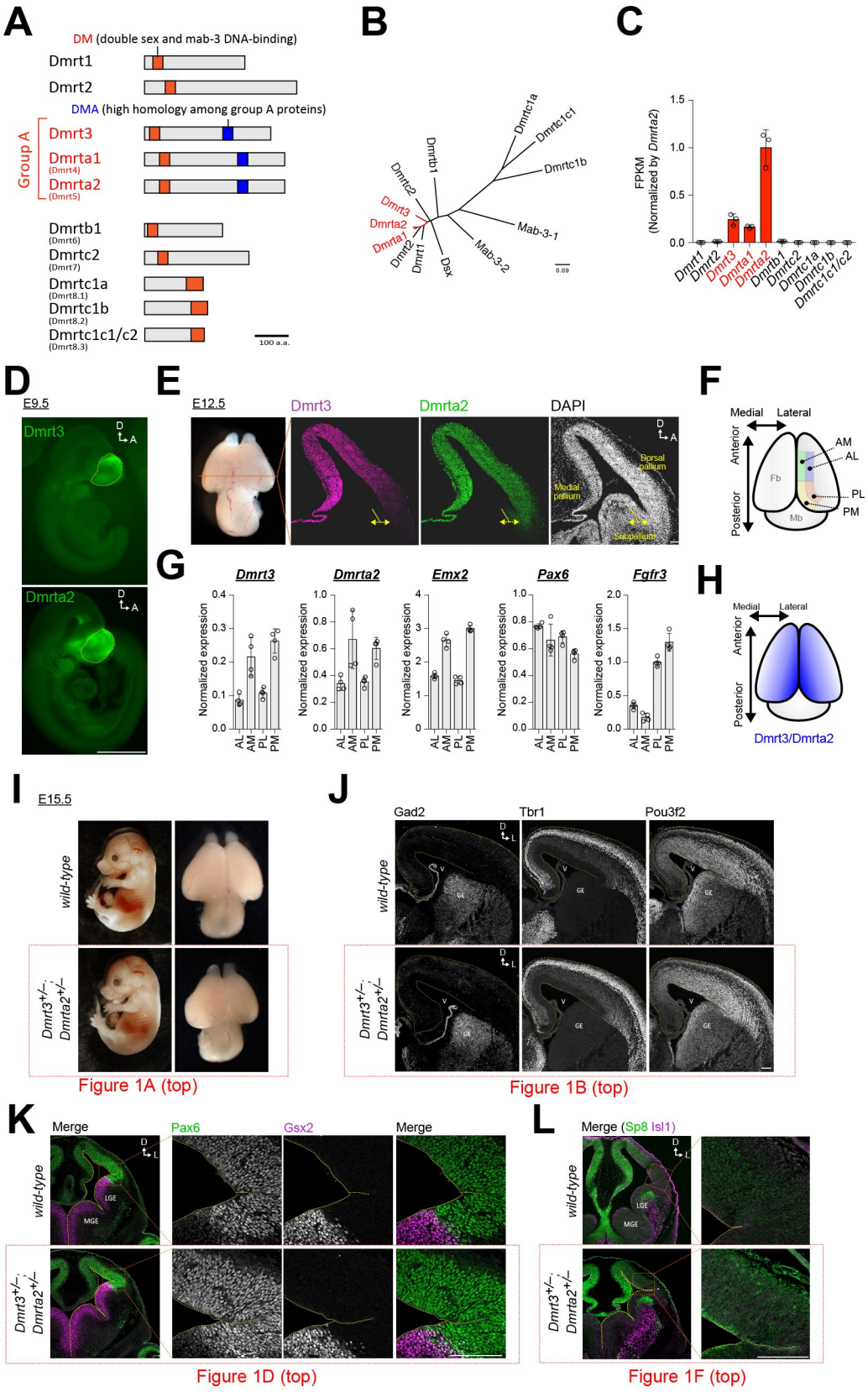

Figure 1A (top)

Figure 1B (top)

Figure 1D (top)

Figure 1F (top)

Figure S1. Graded expression of Dmrt3 and Dmrta2 in the developing cerebral cortex of mice.

A, Schematic illustration of the domain structure of mouse Dmrt proteins. The three Dmrt proteins (Dmrt3, Dmrta1, and Dmrta2) are subcategorized as Dmrt "A" family proteins due to their conserved DMA domain. **B,** Molecular phylogenic tree for the DM domains of ten mouse Dmrt proteins, the Drosophila double sex (dsx) protein, and the C. elegans mab-3 protein. **C,** Relative gene expression of *Dmrt* genes in the dorsal telencephalon at E14.5, as analyzed by deep sequencing. The values are represented as relative value to the *Dmrta2* expression. **D,** Whole-mount immunofluorescence for Dmrt3 and Dmrta2 in E9.5 mouse embryos. Scale bars, 1 mm. **E,** Immunofluorescence for Dmrt3 and Dmrta2 in coronal sections of the mouse telencephalon at E12.5. Scale bars, 50 μm. **F,** Schematic showing four subdivided areas of the dorsal telencephalon for which gene expression was examined as in (G). AL, anterior-lateral; AM, anterior-medial; PL, posterior-lateral; PM, posterior-lateral. **G,** Expression of *Dmrt3*, *Dmrta2*, and marker genes expressed in a gradient in the developing telencephalon. Expression is normalized against *Sox2*, as analyzed by qPCR in the four brain regions indicated in (F). The error bars represent ±s.d. (n=4 per group). **H,** Schematic summarizing the graded expression of Dmrt3 and Dmrta2 in the developing mouse dorsal telencephalon. **I,** Lateral views (left) and top views of the forebrain (right) of E15.5 wild-type and *Dmrt3/Dmrta2* double heterozygous embryos. **J,** Immunofluorescence for Gad2, Tbr1, and Pou3f2 in coronal sections of the telencephalon in the wild-type and *Dmrt3/Dmrta2* double heterozygous E15.5 embryos. **K,** Immunofluorescence for Pax6 and Gsx2 in coronal sections of the telencephalon of wild-type and *Dmrt3/Dmrta2* double heterozygous E12.5 embryos. **L,** Immunofluorescence for Sp8 and Isl1 in coronal sections of the telencephalon of wild-type and *Dmrt3/Dmrta2* double heterozygous E12.5 embryos. In (K) and (L), the right panels represent higher magnifications of the boxed regions indicated in the left panels.

D, dorsal; L. lateral; A, anterior; V, ventricle; LGE, lateral ganglionic eminence; MGE, medial ganglionic eminence. In all immunofluorescence images, the yellow dotted lines indicate the ventricular surface. Scale bars, 100 μm.

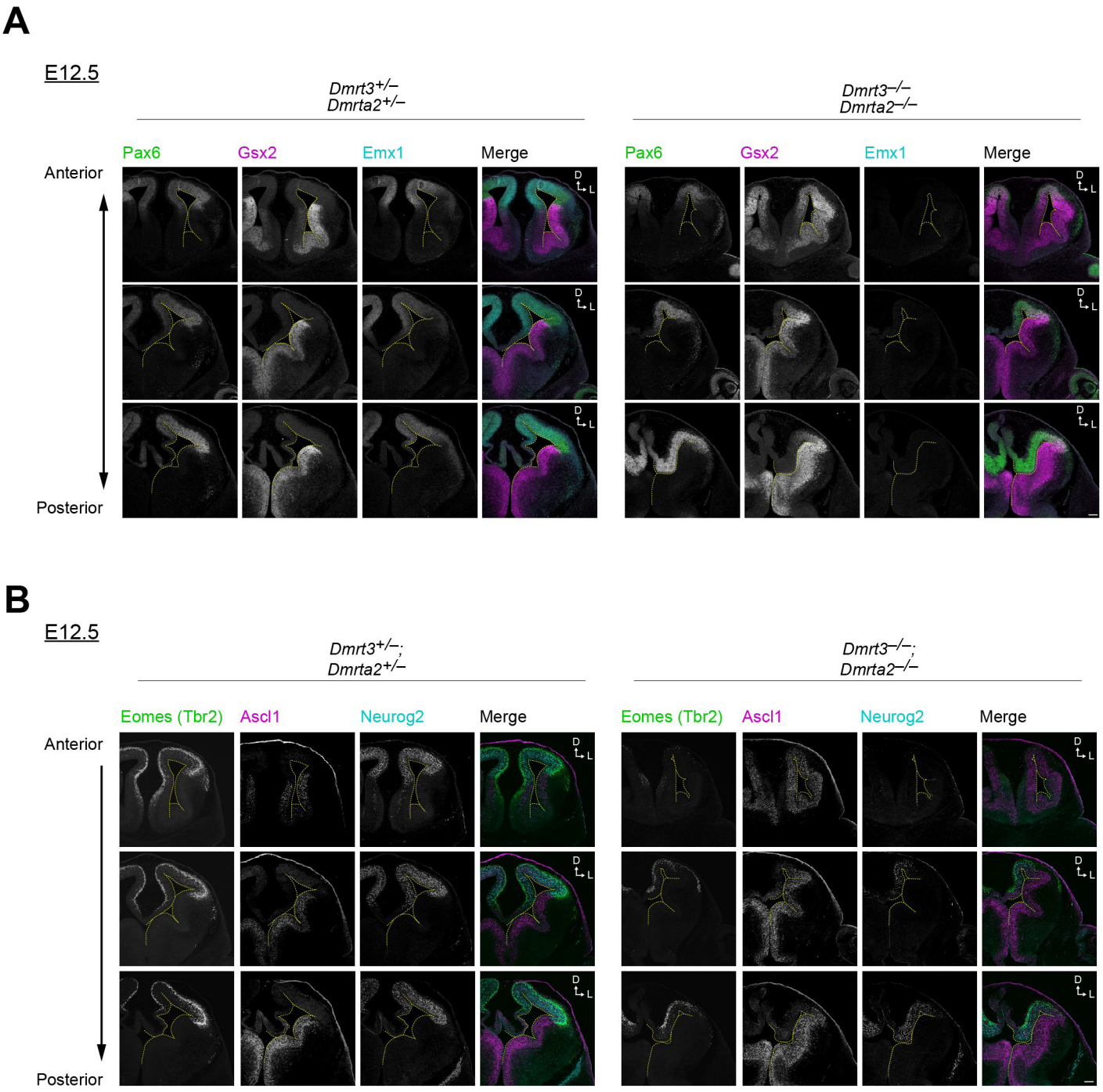

Figure S2. Aberrant expression of transcription factors involved in cerebral cortical development.

A, B, Immunofluorescence for Pax6, Gsx2, and Emx1 (A), or Ascl1, Eomes (Tbr2), and Neurog2 (B), in coronal sections across the anteroposterior telencephalon of *Dmrt3/Dmrta2* mutant E12.5 embryos. The images are aligned along the anteroposterior axis from top to bottom. The dotted lines indicate the ventricular surface. Scale bars, 100 μm.

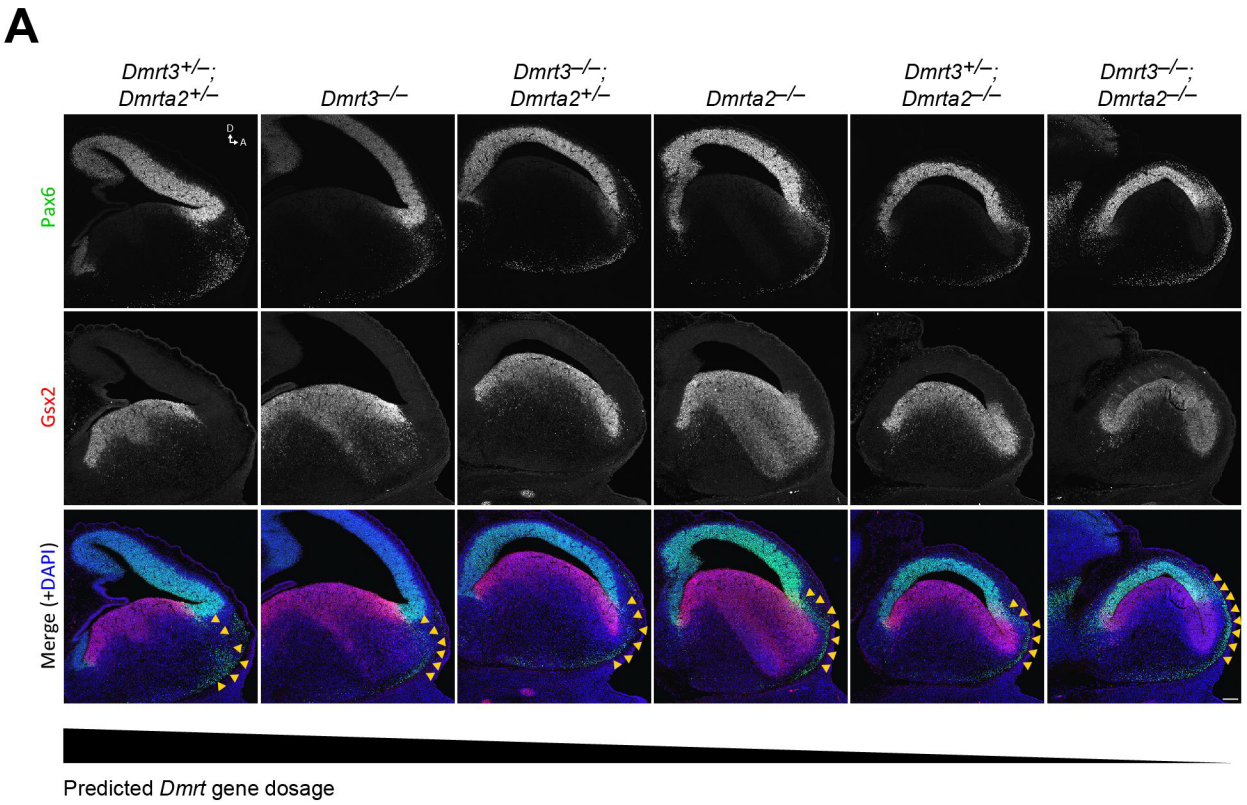

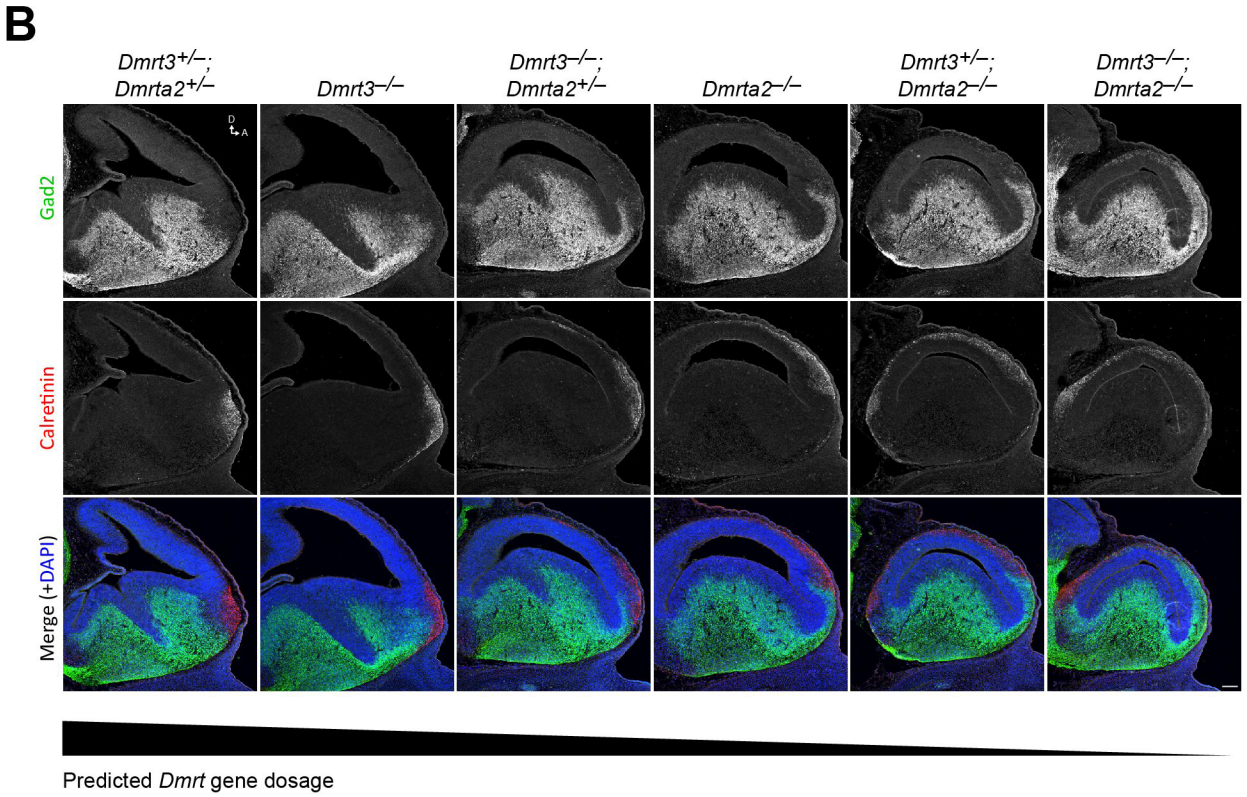

Figure S3. Gene dosage-dependent suppression of GABAergic neuron production and the expression of Gsx2 by Dmrt factors.

A, B, Immunofluorescence for Pax6 and Gsx2 (A), or Gad2 and Calretinin (B), in sagittal sections of the telencephalon of E12.5 *Dmrt* mutant embryos. The yellow arrowheads in (A) indicate the pax6-positive-migrating olfactory bulb interneurons. Scale bars, 100 μm.

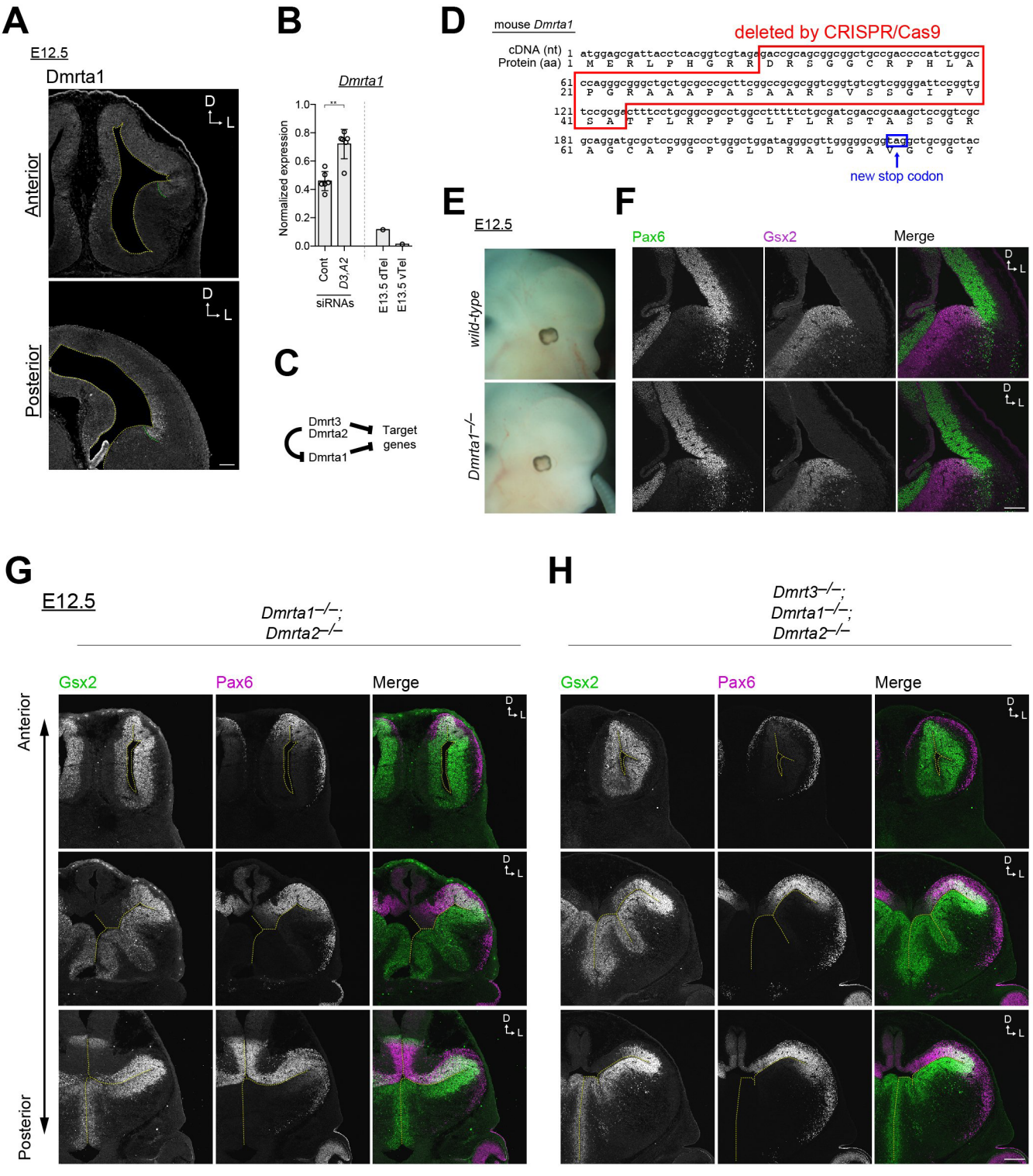

Figure S4. Double or triple mutants for *Dmrt* genes, including *Dmrta1*, phenocopies mutants for *Dmrt3* and *Dmrta2*.

A, Dmrta1 immunofluorescence in coronal sections from the anterior and posterior E12.5 mouse telencephalon. **B,** Gene expression of *Dmrta1* normalized to *Sox2* as analyzed by qPCR in cells electroporated with control siRNAs those targeting *Dmrt3* and *Dmrta2*. The error bars represent ±s.d. (n=6 per group). The statistical significance was determined using Student's t-test with Welch's correction (**p<0.01). **C,** The possible regulatory mechanism for *Dmrta1* expression. **D,** Confirmation of successful CRISPR/Cas9-mediated deletion of the genomic sequence around the *Dmrta1* start codon in ES cells. These ES cells were used to generate *Dmrta1* knockout mutant mice. **E,** Lateral views of the head of E12.5 *Dmrta1* mutant embryos. **F, G, H,** Immunofluorescence for Pax6 and Gsx2 in coronal sections across the anteroposterior telencephalon of E12.5 *Dmrta1* single mutant (F), *Dmrt3/Dmrta2* double mutant (G), and *Dmrt3/Dmrta2/Dmrta1* triple mutant (H) embryos. The images are aligned along the anteroposterior axis from top to bottom. The dotted lines indicate the ventricular surface. Scale bars, 100 μm.

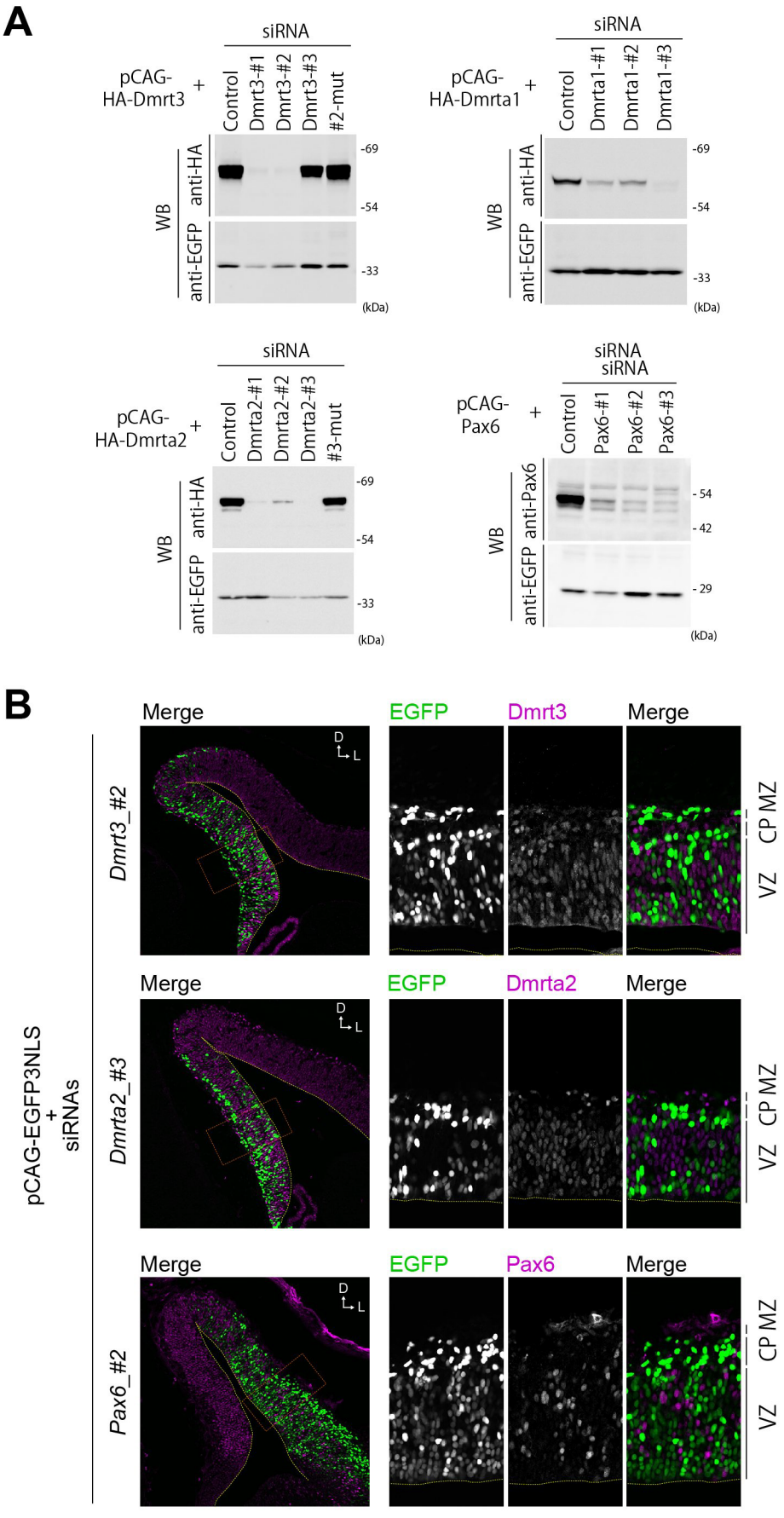

Figure S5. Efficient knockdown of target genes in the developing cerebral cortex via *in utero* electroporation of siRNAs.

A, Evaluation of the knockdown efficiency of siRNAs against indicated *Dmrt* genes or Pax6 by western blotting using HEK293 cells. **B,** Confirmation of an effective knockdown of endogenous protein expression via siRNA transfection into neural progenitors using *in utero* electroporation. Immunofluorescence was performed for Dmr3, Dmrta2, and Pax6 in brains electroporated with siRNAs targeting *Dmrt3*, *Dmrta2*, and *Pax6*, respectively. Right panels represent higher magnifications of the boxed regions indicated in the left panels.

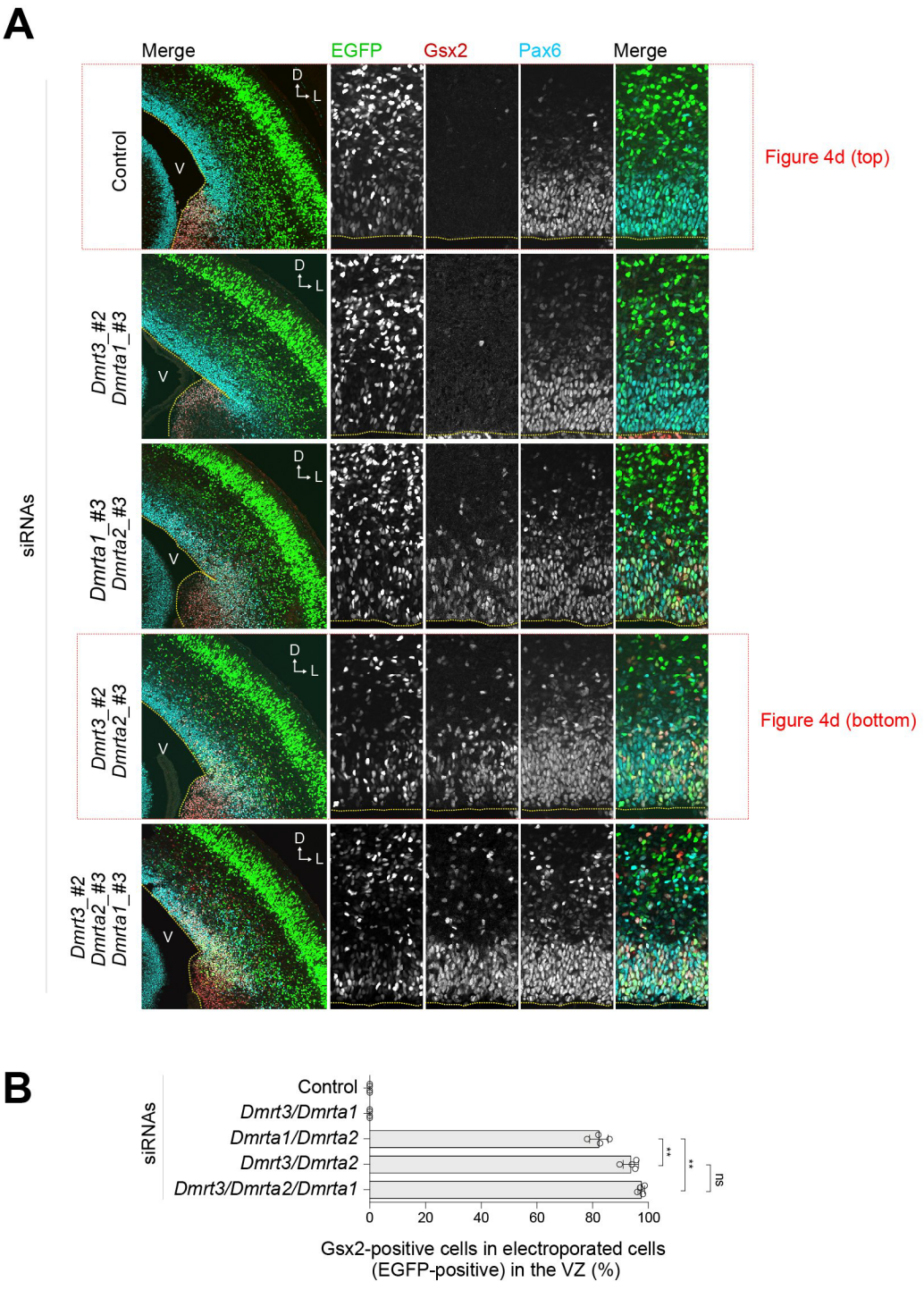

Figure S6. Acute knockdown of *Dmrt* genes phenocopies *Dmrt3* and *Dmrta2* double mutants.

A, Immunofluorescence for Gsx2 and Pax6, as well as EGFP fluorescence, in coronal sections of an E15.5 mouse telencephalon electroporated with the indicated combinations of siRNAs targeting *Dmrt3*, *Dmrta1*, and *Dmrta2*. **B,** The quantification of Gsx2-positive cells that emerged ectopically in the dorsal telencephalon following the knockdown of *Dmrt* genes. All of the error bars represent ±s.d. (n=4 per group). The statistical significance was determined using Student's t-test with Welch's correction (ns, not significant; **p<0.01).

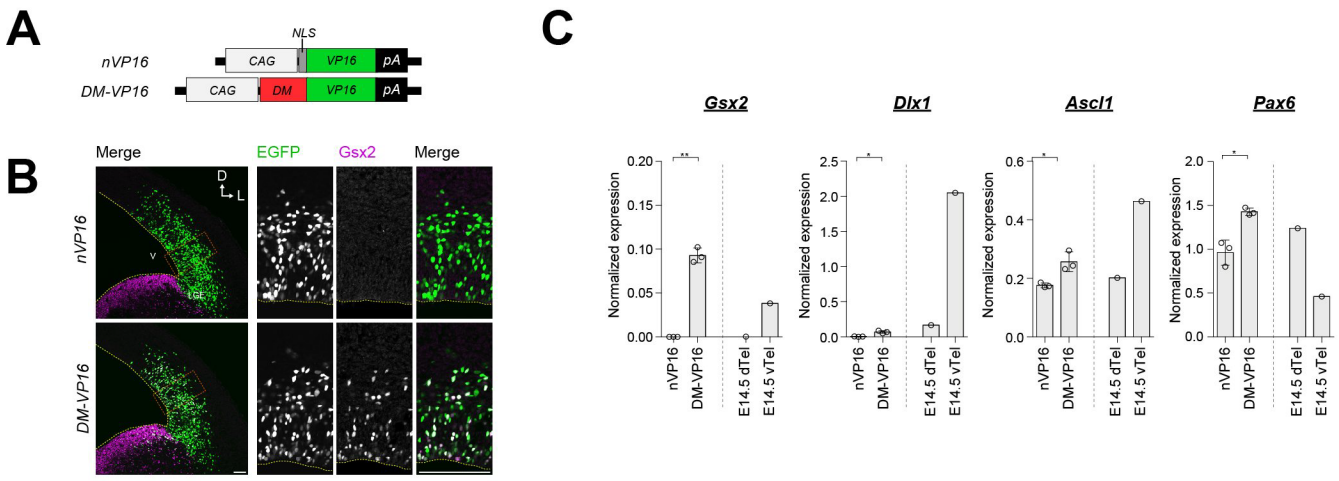

Figure S7. Overexpression of the VP16-fused DM domain in the dorsal telencephalon induces ectopic expression of Gsx2.

A, Structure of the expression plasmid for overexpressing the DM domain of Dmrt3 fused to the VP16 transactivation domain under the control the *CAG* promoter. Nuclear localization signal (NLS) fused to VP16 was used as control. **B,** Immunofluorescence for Gsx2, as well as EGFP fluorescence, in coronal sections of an E13.5 mouse telencephalon electroporated with the expression plasmid indicated in (A) at E12.5. **C,** Gene expression of *Gsx2, Dlx1*, *Ascl1*, and *Pax6* normalized to *Sox2* in the nVP16- (lane 1) and DM-VP16-transfected cells (lane 2), as determined using qPCR. All of the error bars represent ±s.d. (n=3 per group). The statistical significance was determined using Student's t-test with Welch's correction (*p<0.05; **p<0.01).

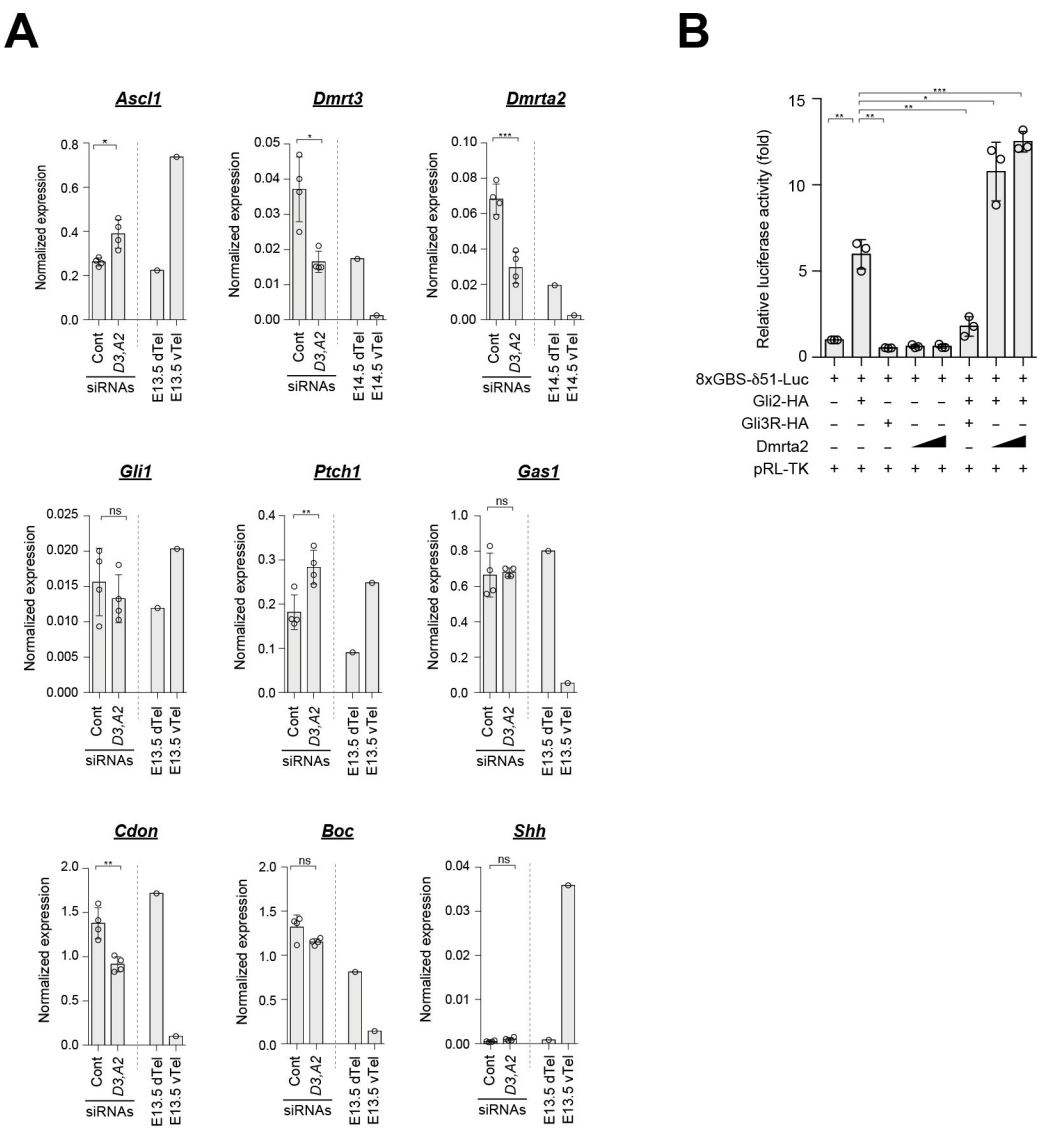

Figure S8. Dmrt factors do not affect the Shh signaling pathway.

A, Expression of Shh-signaling related genes, including *Ascl1*, *Dmrt3*, *Dmrta2*, *Gli1, Ptch1*, *Gas1*, *Cdon*, *Boc*, and *Shh* normalized to *Sox2* in control (lane 1) or double knockdown (*D3, A2*; lane2) cells, as determined using qPCR. The error bars represent ±s.d. (n=4 per group).

B, Influence of Dmrt expression on the transcriptional activation or repression of an 8× Gli binding sequence (8xGBS-δ51-Luc) by Gli2 or Gli3R (a repressor form of Gli3). The error bars represent ±s.e.m. (n=4 per group).

The statistical significance was determined using Student's t-test with Welch's correction (ns, not significant; *p<0.05; **p<0.01; ***p<0.001).

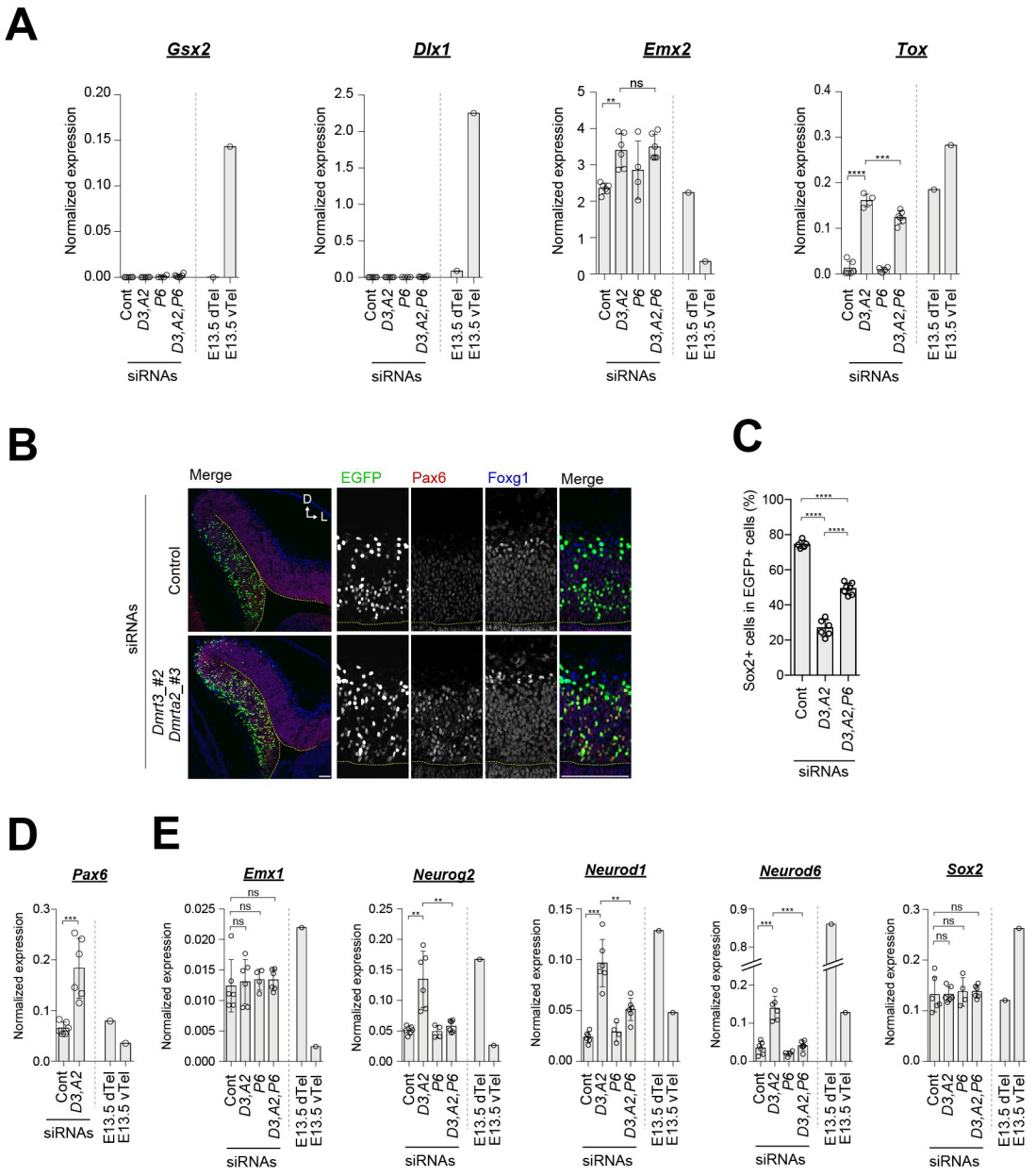

Figure S9. Genetic interaction between *Dmrt* factor genes and *Pax6*.

A, Gene expression of *Gsx2, Dlx1 Emx2,* and *Tox* normalized to *Sox2* in the electroporated cells, as determined by qPCR. The error bars represent ±s.d. (n=6 per group). **B,** Immunofluorescence for Pax6 and foxg1, as well as EGFP fluorescence, in coronal sections of an E13.5 mouse telencephalon electroporated with control siRNAs or siRNAs targeting *Dmrt3* and *Dmrta2*. **C,** The quantification of Sox2-positive neural progenitors in the electroporated cells at E13.5. The error bars represent ±s.d. {n=5 (cont), n=6 (*D3,A2*), n=7 (*D3,A2, Pax6*)}. **D, E,** Gene expression of *Pax6 (D), Emx1 (E), Neurog2 (E), Neurod1 (E)* and *Neurod6 (E)* normalized to *Gapdh* in the electroporated cells, as analyzed by qPCR. The error bars represent ±s.d. {n=6 per group in (E), n=6 per group in (F)}.

The statistical significance in (A), (C), (D), and (E) was determined using Student's t-test with Welch's correction (ns, not significant; **p<0.01; ***p<0.001; ****p<0.0001).

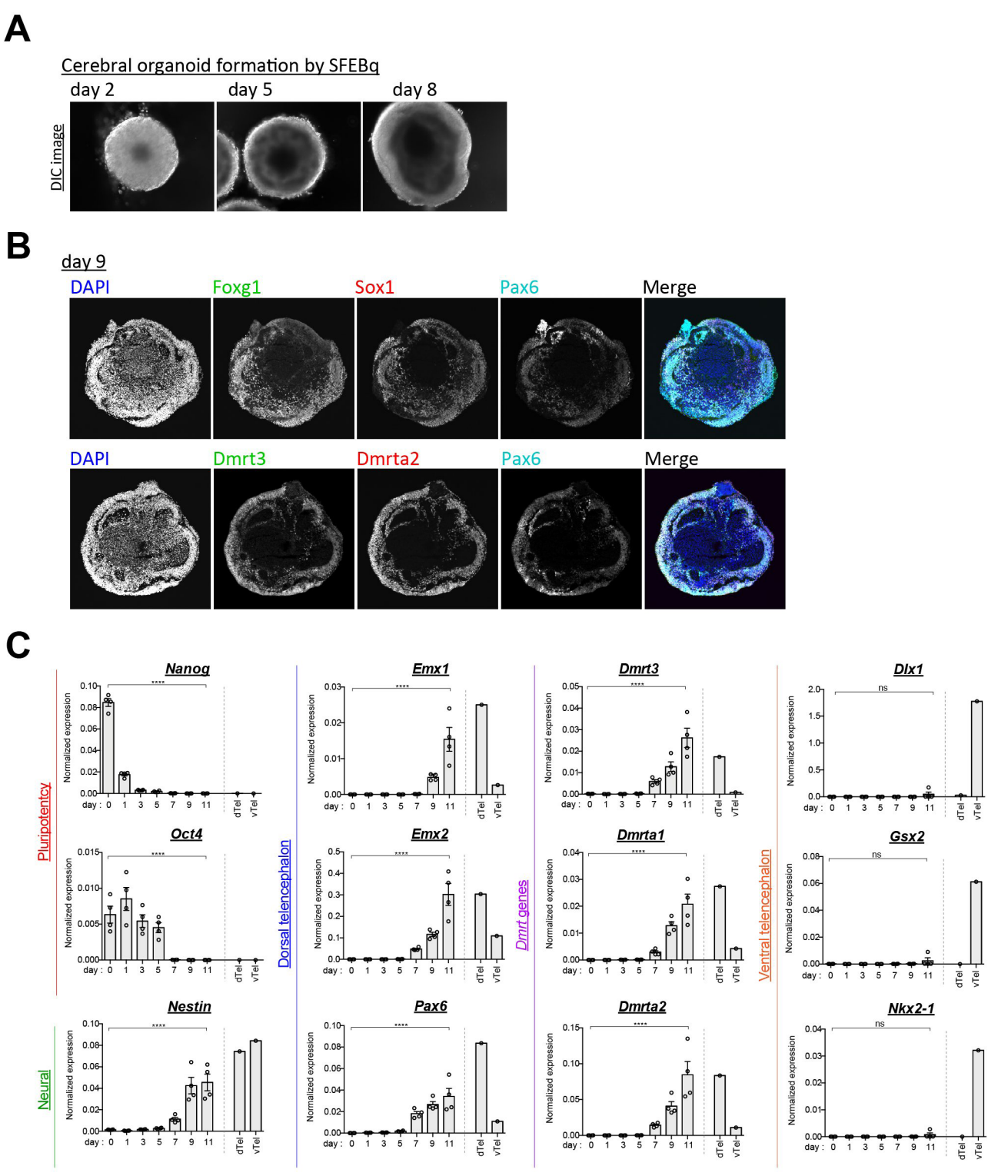

Figure S10. Formation of cerebral organoids from mouse ES cells.
A, DIC images of cell aggregates established using SFEBq-mediated formation of cerebral organoids on day 2, 5, and 8. **B,** Immunofluorescence for Foxg1, Sox1, Pax6, Dmrt3, and Dmrta2 in cerebral organoids on day 9. **C,** Gene expression of marker genes for pluripotency (*Nanog* and *Oct4*), neural fate (*Nestin*), dorsal telencephalic fate (*Emx1*, *Emx2*, and *Pax6*), the *Dmrt-A* gene family (*Dmrt3*, *Dmrta1*, and *Dmrta2*), and the ventral telencephalic fate (*Dlx1*, *Gsx2*, and *Nkx2-1*) normalized to *Gapdh*. The error bars represent ±s.e.m. (n=4 per group). The statistical significance was determined using one-way ANOVA (ns, not significant; ****p<0.0001).

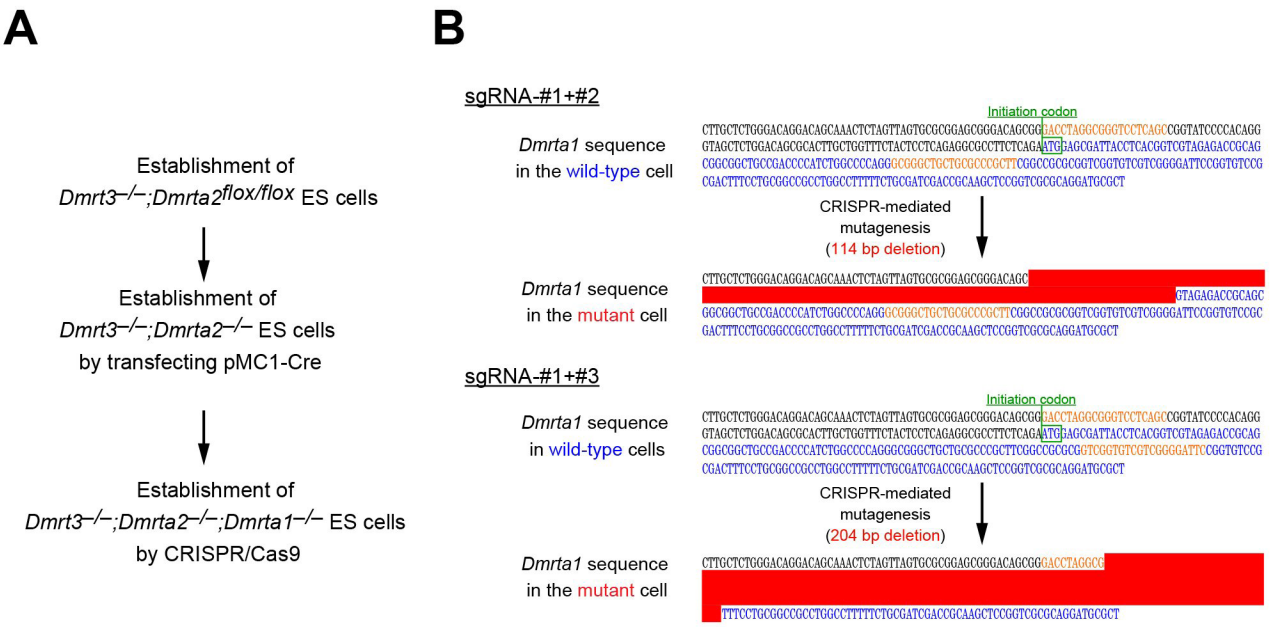

Figure S11. Establishment of the *Dmrt3/Dmrta2/Dmrta1*-mutant ES cells.

A, Schematic summarizing the establishment of the *Dmrt*-mutant ES cells. The *Dmrt3-/-,Dmrta2flox/flox* ES cells were prepared first, and the *Dmrta2* gene was deleted subsequently to isolate *Dmrt3/Dmrta2* mutant ES cells by transfecting with an expression plasmid encoding Cre recombinase. The *Dmrt3, Dmrta1*, and *Dmrta2* triple knockout ES cells were established using *Dmrt3/Dmrta2* DKO ES cells by transfecting CRISPR/Cas9 plasmids targeting *Dmrta1*. **B,** Confirmation of successful CRISPR/Cas9-mediated deletion of the genomic sequence near the *Dmrta1* start codon in *Dmrt3/Dmrta2* DKO ES cells. Two sets of guide RNA sequences were used independently to establish the mutant cells. The DNA sequences indicated in blue and orange represent the open reading frame (ORF) of *Dmrta1* and the CRISPR/Cas9 target sequences, respectively.

Table S1

Primers for RT-qPCR

Gene	Forward (5'-3')	Reverse (5'-3')	Reference
Gapdh	TGACCACAGTCCATGCCATC	GACGGACACATTGGGGGTAG	Kamiya et. al., 2011
Sox2	CATGAGAGCAAGTACTGGCAAG	CCAACGATATCAACCTGCATGG	Kawaguchi et. al., 2008
Nestin	CTCCTGGAACCCTGTTCACC	AGTGCTTCAGTCCCAGCTTC	Primer-BLAST
Tox	CACAAGTTGTCACCCAAGCG	TACAGCGCTTTGTCCCTCTG	Primer-BLAST
Pax6	GGAGAGAGCATGTGATCGAG	TGAAGTGCTTCTAACCGCCA	Primer-BLAST
Neurog2	GTCAAAGAGGACTATGGCGTGTG	TACAGTCTTACGAGGTTCCCCACG	Kawaguchi et. al., 2008
Ascl1	GCCTCCATTGAAGCAACGTC	AGAAGCAAAGACCGTGGGAG	Primer-BLAST
Gsx2	GACCCACGGAGATTCCACTG	CGCTGTCCTCATCCTTTTGC	Primer-BLAST
Nkx2-1	TTCTGAAGCCGAAGTATCCA	ACGGAGTCGTGTGCTTTGG	Tucker et. al., 2008
Dlx1	TCCGAGAAGAGTACGGTGGT	ACTTGGAGCGTTTGTTCTGG	Lo Iacono et. al., 2008
Neurog2	GTCAAAGAGGACTATGGCGTGTG	TACAGTCTTACGAGGTTCCCCACG	Kawaguchi et. al., 2008
Neurod1	ACAGACGCTCTGCAAAGGTTT	GGACTGGTAGGAGTAGGGATG	Primer-BLAST
Neurod6	CACGTTCGTCCAAAACTTATGC	GAATGTGGAGTAGGGTGACCT	Primer-BLAST
Fgfr3	AAGCCAGCCAGCTGCACACA	TCAAACGGCACGGAGAGGTCCA	Boroviak et. al., 2014
Dmrt3	TGCCAACCGACTATGAGCAGGGA	TGTCTCTGAAAACGGCCCGAGC	Kawaguchi et. al., 2016
Dmrta1	ACTGGTTCCAGCATTGCCTT	GGACGGCTCCCTAATCATCC	Primer-BLAST
Dmrta2	CGTTGCGGTATTTGTCGCTC	ACTCACACTGCACCAAGGAA	Primer-BLAST
Dmrt3 (detecting knockdown)	CTACCGCCTCGCAGTCGTC	CGCAGTGTTGTCCGTGGAAC	Primer-BLAST
Dmrta2 (detecting knockdown)	CGGCCTGCCTACGAAGTCT	TCGGGCGACAAGGGCTTC	Primer-BLAST
Gas1	CCTCTGCACCACGTGTCTTA	CCTAGATGGCAGTACCGAGC	Primer-BLAST
Cdon	GTCGGAATTGCCGGAACAAC	GGGGCTTCATTTCCAGACCA	Primer-BLAST
Boc	GATTGAAGTAGACGAGGGGAAC	GATGGCATGATCAGGTAGTTGT	Lee et. al., 2010
Gli1	CCAAGCACCAGAATCGGACC	ACTGTCTTCACGTGTTTGCG	Primer-BLAST
Ptch1	CTATCCATCAGCGTGGTGCT	AATGAGGCCCATCATGCCAA	Primer-BLAST
Emx1	ATATCAACCGGTGGCGCATC	GCCCTTGTGGGCTCTTGATT	Primer-BLAST
Emx2	ATTGCTACCAAGCAGGCGAG	TCTTGCTCTGTGCTGTCCATT	Primer-BLAST
mKO2	CTCCGTCAATGGGCATGAGT	GCGCAGTGTCATCTCCTGAT	Primer-BLAST
NesE-TetON-A2	TACGCCTTCAGCGACCTCAT	AGATCCGGTGGATCCCATAC	Primer-BLAST

Primers for ChIP-qPCR

Target gene	Forward (5'-3')	Reverse (5'-3')	Reference
Pax6-A	CAGAGCCGGGTTAGAGAAGG	GAGCGACAGGATTGTTCCCA	Primer-BLAST
Pax6-B	ATGGGAACAATCCTGTCGCT	GTCTCCTTCAGCTAGACGCT	Primer-BLAST
Pax6-C	TATGTTTCCTTAACTTGTTGTCTGTTTG	AAGCCCCAGCACCTACCTGTGCATACC	Primer-BLAST
Pax6-D	AGGCTGGTTACTTATTGTCCTGACAC	TCATTAGATTATACTGGTCGGCAGAGAC	Primer-BLAST
Gsx2-A	TGTACAGTAATTAACAGCTCTTGACTG	AGGGTCCCTGTTAGGGATATTTAATC	Primer-BLAST
Gsx2-B	ACTTTAAACAGGCTCCACATGCATG	TGCTAATGGCTGGAATATAGTTAGAATTG	Primer-BLAST
Gsx2-C	CTGGAGGGAGACGCGTTTAG	TCCTCCCTTTTCAGCTTGCC	Primer-BLAST
Gsx2-D	CCTGCCAATCAACCAAGGGA	AGTTCTCCAGCACTTGCCTC	Primer-BLAST